JGR Oceans

RESEARCH ARTICLE
10.1029/2020JC016771

# Shifting Sediment Dynamics in the Coos Bay Estuary in Response to 150 Years of Modification

**E. F. Eidam[1], D. A. Sutherland[2], D. K. Ralston[3], T. Conroy[4], and B. Dye[5]**

[1]Department of Marine Sciences, University of North Carolina at Chapel Hill, Chapel Hill, NC, USA, [2]Department of Earth Sciences, University of Oregon, Eugene, OR, USA, [3]Woods Hole Oceanographic Institution, Woods Hole, MA, USA, [4]School of Science, University of Waikato, Hamilton, New Zealand, [5]Department of Coastal Systems, Royal Netherlands Institute for Sea Research, AB Den Burg, Netherlands

**Abstract** Estuaries worldwide have experienced modifications including channel deepening and intertidal reclamation over several centuries, resulting in altered fine sediment routing. Estuaries respond differently based on preexisting geometries, freshwater and sediment supplies, and extents and types of modification. The Coos Bay Estuary in Oregon is a relatively small estuary with complex geometry that has been extensively modified since 1865. A sediment transport model calibrated to modern conditions is used to assess the corresponding changes in sediment dynamics. Over ~150 years, channel deepening (from ~6.7 to 11 m), a 12% increase in area, and a 21% increase in volume have led to greater tidal amplitudes, salinity intrusion, and estuarine exchange flow. These changes have reduced current magnitudes, reduced bed stresses, and increased stratification, especially during rainy periods. Historically, fluvially derived sediment was dispersed across broad, deltaic-style flats and through small tidal channels. Now, river water and sediments are diverted into a dredged navigation channel where an estuarine turbidity maximum (ETM) forms, with modeled concentrations >50 mg/L and measured concentrations >100 mg/L during discharge events. This "new" ETM supplies sediment to proximal embayments in the middle estuary and the shallow flats. Overall, sediment trapping during winter (and high river discharges) has increased more than two-fold, owing to increased accommodation space, altered pathways of supply, and altered bed stresses and tidal asymmetries. In contrast to funnel-shaped estuaries with simpler geometries and river-channel transitions, these results highlight the importance of channel routing together with dredging in enhancing sediment retention and shifting pathways of sediment delivery.

**Plain Language Summary** Estuaries worldwide are commonly dredged to accommodate development. Related modifications, including dumping of dredge spoils, construction of jetties, waterfront reclamation, and so on all serve to change the geometry of estuaries. These modifications can result in changes to how water and sediment flow through the estuary. We used a high-resolution model of water and sediment dynamics in the Coos Bay estuary in Oregon, together with modern and historic bathymetric (depth) data from the estuary, to assess how 150 years of modification (dredging and other projects) have altered the storage and transport. Overall, the model results suggest that the estuary now retains more sediment, owing largely to sediment trapping in the deepened navigation channel. This is an effect of changes in how water flows through the system and the additional space created to hold sediment (accommodation space). More nuanced changes have occurred on shallow intertidal flats and in subembayments, which have also led to increased sediment retention

**Key Points:**

- Dredging and other estuarine modifications have altered hydrodynamics and sediment pathways in the Coos Bay Estuary for >150 years
- Rerouting of the river has caused preferential sediment routing into a dredged navigation channel, where a turbidity maximum now forms
- Based on modeling of historic and present conditions, the estuary now retains more sediment, in channels, flats, and embayments

**Supporting Information:**

- Supporting Information S1
- Movie S1

**Correspondence to:**
E. F. Eidam,
efe@unc.edu

**Citation:**
Eidam, E. F., Sutherland, D. A., Ralston, D. K., Conroy, T., & Dye, B. (2021). Shifting sediment dynamics in the Coos Bay Estuary in response to 150 years of modification. *Journal of Geophysical Research: Oceans*, *126*, e2020JC016771. https://doi.org/10.1029/2020JC016771

Received 4 SEP 2020
Accepted 2 DEC 2020



## 1. Introduction

Estuaries serve as effective sediment traps and critical interfaces between rivers and the coastal ocean, providing key infrastructure and ecosystem services (e.g., Guerry et al., 2012; Lotze, 2010; Lotze et al., 2006). Because of their prime location at the land-ocean boundary and rich species diversity, estuaries have also seen intense development pressure over the past several centuries. While some of this pressure has come in the form of overharvesting local species and degradation of water quality, many ecosystem changes result from physical restructuring of the estuary through dredging, spoils disposal, land reclamation and shoreline armoring, accelerated sediment delivery related to watershed denudation, reduced sediment delivery related to upstream damming and diking, and other sediment-related modifications (Barbier et al., 2011;

Lane, 2004; Van Dyke & Wasson, 2005; van Maren, et al., 2015; Winterwerp et al., 2013). Because of demands related to commercial ship traffic, many estuaries have been dredged, and dredging spoils are commonly dumped on intertidal areas to save on disposal costs and/or to reclaim land (Blott et al., 2006; Familkhalili & Talke, 2016; Nichols & Howard-Strobel, 1991; Talke et al., 2018; Townend et al., 2007).

Changes in estuarine bathymetry and upstream sediment supply alter estuarine sediment dynamics, including changes in sediment erosion/deposition patterns, changes in water quality and clarity, and changes in seabed grain-size, which can impact the benthic environment. Over the past several decades, observational studies have yielded a wealth of insight to estuarine sediment dynamics, including the development of an estuarine turbidity maximum (ETM) at the freshwater/saltwater intersection (or at locations dictated by bathymetric changes), flocculation processes, and changes in seabed texture and erodibility over timescales from tidal to seasonal (Burchard et al., 2018; Jay et al., 2015; Ralston et al., 2012). These processes have been incorporated into models of sediment transport in numerous idealized and real estuaries, but assessments of long-timescale (centennial) changes are generally limited to idealized, depth-averaged, width-averaged, and temporally averaged estuary models (e.g., Dijkstra et al., 2019a, 2019b; Nnafie et al., 2019; Ralston & Geyer, 2009), or models that account for hydrodynamics and have not been expanded to include sediment dynamics (e.g., Chant et al., 2018; Familkhalili & Talke, 2016; Ralston & Geyer, 2019), or models that include sediment dynamics over time scales of years but not centuries (van Maren et al., 2016). In order to anticipate future changes in sediment dynamics over the time scales of sea-level rise and engineering modifications, it is useful to conduct high-resolution analyses of how sediment dynamics have changed in the past century.

In this study, we built on an existing model of the Coos Bay hydrodynamics (see Conroy et al., 2020; Eidam et al., 2020) constructed using the Finite Volume Coastal Ocean Model (FVCOM v3.2.1; Chen et al., 2003). We used an adapted version of the USGS community sediment transport model (Warner et al., 2008) within FVCOM to evaluate sediment transport and patterns of deposition within the estuary. To develop a historical context, we also ran the model using a grid constructed from a digitized 1865 bathymetric chart. The results yield insights into the primary forcings for sediment transport within a complex estuary where the balance of shallow and deep regions has shifted toward the latter due to dredging and intertidal reclamation over the past 150 years. We explore how changes in hydrodynamics including tidal amplitude and salt-wedge propagation have altered the routing and storage of sediment in the system, as well as implications for species which rely on access to suitable substrates and adequate water clarity for success.

## 2. Regional Setting

The Coos Bay Estuary in Oregon is one of the largest estuaries on the US west coast, with a total area of 54 $km^2$ (Rumrill, 2006). Freshwater sources include more than 13 small rivers and creeks. The Coos River is the largest source, supplying ~1 $m^3/s$ during summer and >300 $m^3/s$ during winter rain events (Coos Watershed Association, www.cooswatershed.org). These streams drain the Coast Range, a relatively low-relief region characterized by abundant logging and limited agriculture. In the 1970s, >80% of the Coos River drainage was timberland (Percy et al., 1974). The communities of Coos Bay, North Bend, and Charleston serve as bases for commercial fishing and international shipping.

Coos Bay is an incised river valley which was has been inundated since the Last Glacial Maximum. The main channel of the estuary wraps around a north-south trending anticline and terminates in several long tributary channels/embayments (Isthmus Slough, Catching Slough, Haynes Inlet, and the Coos River). Near the entrance of the bay, the largest tributary embayment, South Slough, extends southward into a syncline. The estuary is net aggradational, and sediments are supplied by streams, littoral drift, aeolian processes, and erosion of sandstone cliffs in South Slough (Baker, 1978; Roye, 1979). In South Slough, accumulation rates on a 0.9-m-deep flat were estimated at 2.3–9 mm/yr over a 300-year timescale (Johnson et al., 2019), greater than the local relative rate of sea-level rise of 1.10 ± 0.73 mm/yr (Komar et al., 2011).

Approximately 25 $km^2$ of the estuary in South Slough has been designated as a National Estuarine Research Reserve and has remained relatively unaltered by construction projects and been managed for long-term habitat health, research, and education. In contrast, the main estuary has experienced a long history of channel deepening and spoils disposal in shallow areas (Beaulieu & Hughes, 1975; Borde et al., 2003;

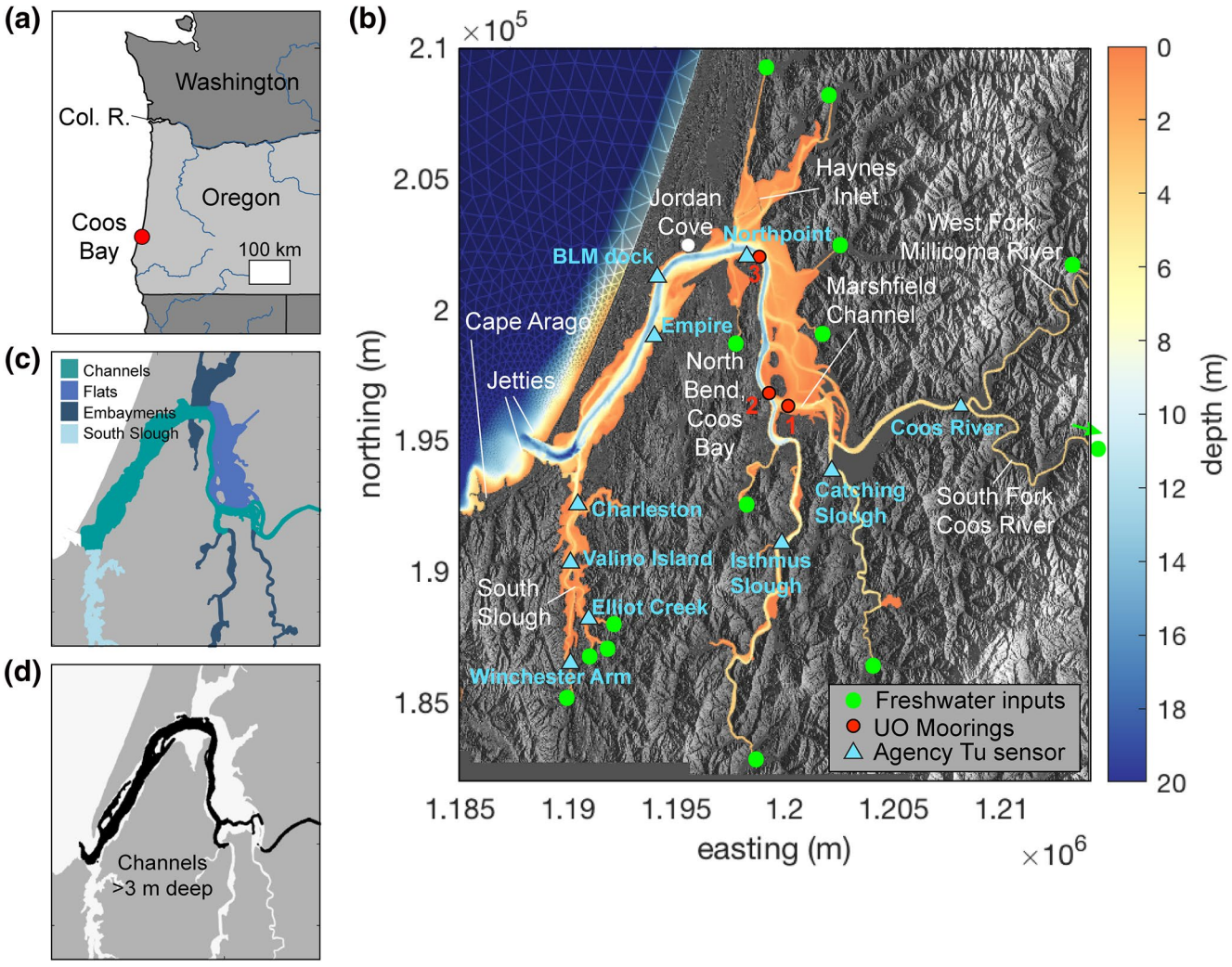


**Figure 1.** Vicinity map. (a) Location of Coos Bay on the Oregon Coast. (b) Topography and bathymetry of the Coos Bay system, highlighting freshwater input nodes used in the model and major rivers, channels, and embayments. Red circles denote three moorings deployed in early 2018, and blue triangles denote 10 turbidity (Tu) sensors deployed by SSNERR. (c) Four subregions (channels, flats, embayments, and South Slough) used in calculations of sediment budgets. (d) Regions of the primary channel and Coos River >3 m deep, used to distinguish hydrodynamic and sediment deposition processes occurring in the navigation channel from other shallow regions of the estuary.

Brophy, 2017; Caldera, 1995; Dicken et al., 1961; Hoffnagle & Olson, 1974; Ivy, 2015). Development activities since the mid-1800s have nearly doubled the cross-sectional area of the estuary entrance, increased the primary navigation depth from ~6.7 to 11 m, increased the total estuarine volume by 21%, and decreased the total estuarine area by 12% (Eidam et al., 2020; Figure 2). The decrease in total area has resulted in a shift from 55% intertidal flats plus wetlands in 1863 to 52% in 1995 (Borde et al., 2003). Much of this change occurred due to dumping of dredge spoils and construction of waterfront infrastructure including an airport runway. Additional changes have included construction of a harbor and bridge at the entrance to South Slough, and diversion of the mouth of the Coos River at the point of entry into the estuary, from a more northerly route to a more westerly route, a change which has partially disconnected it from the broad east-estuary flats (Beaulieu & Hughes, 1975; Eidam et al., 2020; Figure 2). A proposed dredging plan is presently under review for the western reach, and would involve deepening the navigation channel from ~11 to 14 m, and widening by ~45 m (see Eidam et al., 2020).

Estuarine transport in Coos Bay is characterized by mesoscale, mixed semidiurnal tides and exchange flow which varies with fortnightly tidal cycles (Baptista, 1989; Conroy et al., 2020). The tidal prism constitutes

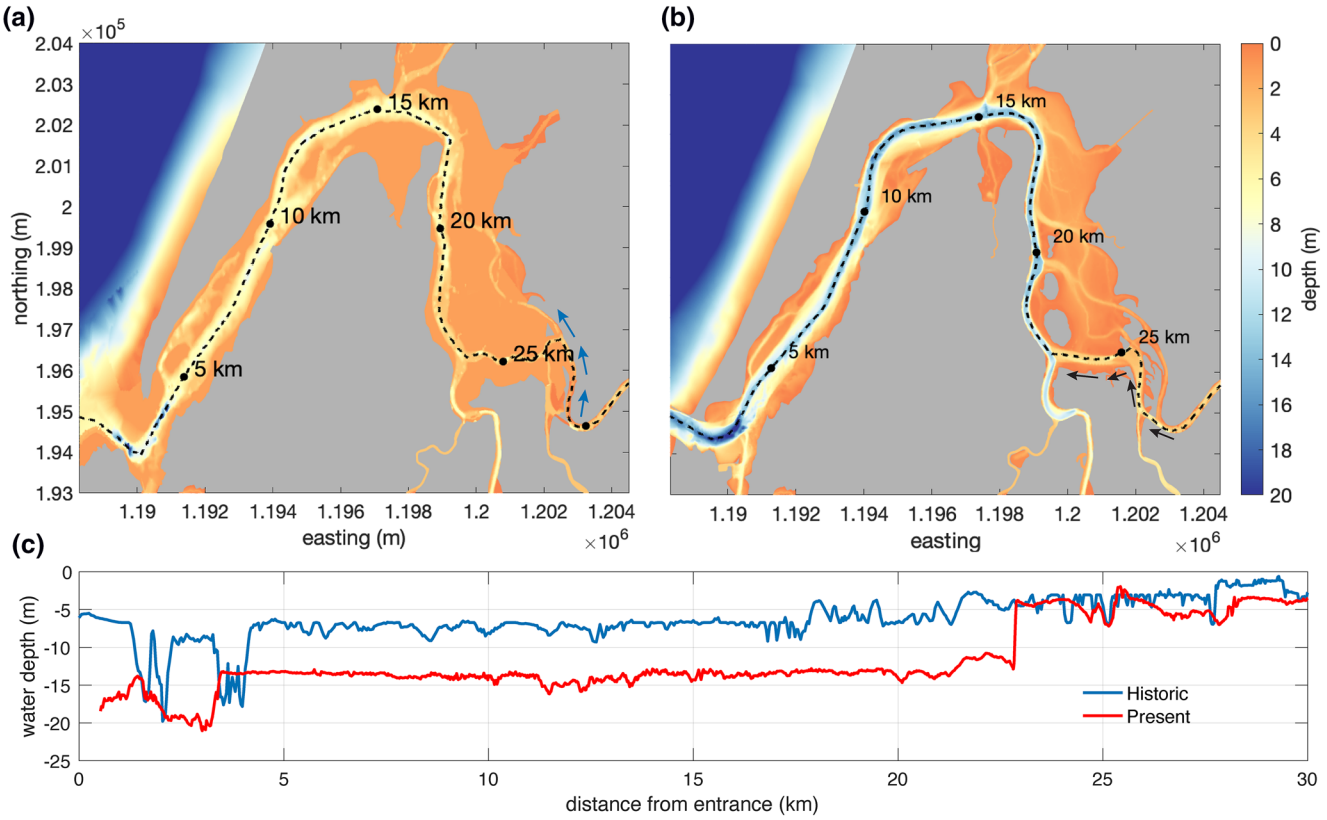


**Figure 2.** Bathymetry: (a) Historical (from 1865 maps), with thalweg outlined and 5-km thalweg distances noted. (b) Modern. (c) Thalweg depth profile, highlighting progressive deepening over time between 0 and 23 km. Arrows in (a) and (b) denote primary discharge path of Coos River, which was across the intertidal flats (historical) and is now routed down Marshfield Channel.

~30% of the estuarine volume (Hickey & Banas, 2003), and the system is well-mixed in summer but strongly stratified in the winter due to freshwater input during rain events (Sutherland & O'Neill, 2016). The increase in depth and volume since 1865 has resulted in a 33% increase in mean tidal amplitude, and 18% increase in salinity intrusion length (Eidam et al., 2020). In map view, the estuary forms an inverted "U" shape, with numerous side embayments (Isthmus Slough, Haynes Inlet, Pony Slough, South Slough) providing additional volume but little to modest freshwater and sediment input (Figure 1). The eastern part of the estuary is dominated by expansive intertidal flats. The head of the estuary terminates at the Coos River (the primary freshwater source), which is presently connected to the dredged navigation channel by Marshfield Channel, which is shallower and experiences limited dredging (Figure 2).

The estuary has historically been home to native oyster species and eelgrass. Recent restoration efforts have focused on reintroducing Olympia oysters (*Ostrea lurida*) after their natural disappearance in the 1700s (Groth & Rumrill, 2009) and enhancing eelgrass habitat. Sediment dynamics in the estuary remain an issue of interest for local environmental managers and regional stakeholders concerned about water quality and estuarine function.

## 3. Methods

### 3.1. Data Collection and Analyses

To establish the baseline conditions for the sediment modeling, observational seabed and suspended-sediment concentrations (SSCs) were measured in situ (2012–2018) and curated from agency reports (2009, 2014). Data from 164 grab samples collected by the US Army Corp of Engineers (USACE; as part of predredging sampling), Oregon State University, and University of Oregon were combined to assess spatial patterns

**Table 1**
*Water-Level and Turbidity Time-Series Data Availability (See Figure 1b for Locations)*

| Site name | Collected by | Longitude | Latitude | Period |
|---|---|---|---|---|
| | **Agency stations** | | | |
| Coos River | SSNERR (SWMP) | −124.1033 | 43.3771 | Oct 2013–Jul 2017 |
| Catching Slough | SSNERR (SWMP) | −124.1731 | 43.3528 | Oct 2013–Jul 2017 |
| Isthmus Slough | SSNERR (SWMP) | −124.2004 | 43.3278 | Oct 2013–Jul 2017 |
| Northpoint | SSNERR (SWMP) | −124.2227 | 43.4258 | Oct 2013–Jul 2017 |
| BLM dock | CTCLUSI | −124.2785 | 43.4152 | Jan 2008–Sep 2016 |
| Empire | CTCLUSI | −124.2805 | 43.3943 | Jan 2007–Jan 2017 |
| Charleston | SSNERR | −124.3205 | 43.3377 | Apr 2002–Mar 2020 |
| Valino Island | SSNERR | −124.3216 | 43.3172 | Jun 1999–Apr 2020 |
| Elliot Creek | SSNERR | −124.3107 | 43.2965 | May 2012–Apr 2020 |
| Winchester Arm | SSNERR | −124.3203 | 43.2824 | Apr 1995–Jun 2012 |
| | **Moorings** | | | |
| (1) Marshfield channel (near-bed) | University of Oregon | −124.2034 | 43.3744 | Jan 2018–Feb 2018 |
| (2) Main channel (near-bed) | University of Oregon | −124.2120 | 43.3780 | Jan 2018–Feb 2018 |
| (3) North Bend piling (near-bed & near-surface) | University of Oregon | −124.2189 | 43.4293 | Dec 2017–Apr 2018 |

Abbreviations: CTCLUSI, Confederated Tribes of the Coos, Lower Umpqua and Siuslaw Indians; SSNERR, South Slough National Estuarine Research Reserve; SWMP, System-Wide Monitoring Program.

of bed sediment sizes (see Section S3 and Table S3). Turbidity data were obtained from the South Slough National Estuarine Research Reserve (SSNERR) and Confederated Tribes of the Coos, Lower Umpqua and Siuslaw Indians (CTCLUSI; see Table 1, Figure 1b, and Sections S1 and S2).

Between 2012 and 2019, more than 900 conductivity/temperature/depth (CTD) and turbidity profiles were collected in the estuary (primarily in the thalweg between the mouth and Coos River entrance) using a profiling CTD sensor outfitted with an optical backscatter sensor (see Section S2). Moorings were deployed at three sites in the upper estuary for approximately three months in winter 2018 to measure temperature, salinity, turbidity, and water-level variations near bed (moorings 1, 2, and 3) and near the surface (mooring 3) (Table 1; Figure 1b).

**Table 2**
*Physical Properties and Model Parameters for Two Modeled Case Studies*

| | Historic | Modern |
|---|---|---|
| Period of bathymetry data | 1865 | 2011–2017 |
| Estuary area, from charts ($km^2$) | 57.8 | 51.0 |
| Estuary volume, model domain ($m^3$) | $1.39 \times 10^8$ | $1.68 \times 10^8$ |
| Number of grid cells | 191513 | 195392 |
| Number of vertices | 101598 | 103065 |
| Number of sigma layers | 20 | 20 |

*Note*. Additional details are given in Eidam et al. (2020) and Conroy et al. (2020).

### 3.2. Model Implementation

The Finite Volume Community Ocean Model (FVCOM, http://fvcom.smast.umassd.edu/) was used to model the hydrodynamics and sediment dynamics of the Coos Bay Estuary. An unstructured triangular grid comprising more than 100,000 elements with variable horizontal resolution (typically 15 m in the estuary) and 20 vertical sigma layers was developed using a compilation of data available from 2011 to 2017, including existing NOAA survey data, single-beam bathymetry measurements collected from personal watercraft, and airborne bathymetric lidar data (Conroy et al., 2020; Eidam et al., 2020). The hydrodynamic portion of the model is described in detail in Conroy et al. (2020) and the parameters used for the sediment module are described in detail here (Table 2). The model was also run using a historical bathymetric grid derived from digitization of Coast Survey charts published in 1865 (Table 2; see Eidam et al., 2020 for details).

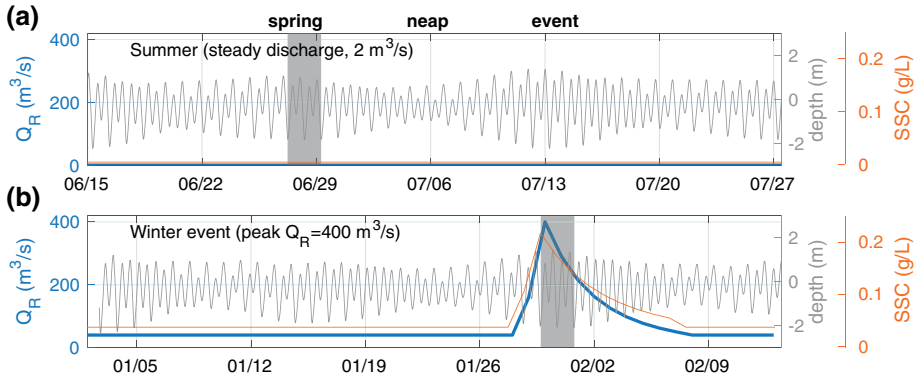


**Figure 3.** Time series of water level in the middle estuary, and model input parameters for three seasonal discharge cases. (a) Summer steady discharge case. (b) Winter high-discharge event case (Coos River discharge peaked at 400 $m^3/s$ during the event; SSC peaked at 215 mg/L). Gray shading highlights 2-day periods used to assess tidally averaged variations in sediment transport and deposition between low and high-discharge periods. (SSC means suspended-sediment concentration).

For both bathymetry cases, the model was run for different seasonal discharge conditions: a summer case with Coos River discharge of 2 $m^3/s$ (Figure 3a), and a winter "event" case with background discharge of 40 $m^3/s$ increasing over 2 days to a peak of 400 $m^3/s$, and decreasing to background levels over 7 days (Figure 3b). In the hydrodynamics-only version of the model (see Eidam et al., 2020), the winter discharge-event case was repeated for neap and spring tides, but here we only consider the spring-tide case in order to examine the most notable signals of sediment transport.

#### 3.2.1. Seabed Sediments

The sediment bed was modeled using five vertical layers and five sediment size classes (Table 2). In order to develop an initial bed condition for the two distinct bathymetric cases, the model was seeded with 45% coarse sand, 45% fine sand, 5% mud, and 5% fine mud in each vertical bed layer, and allowed to run for 93 days with high sand erodibility values (Table 3). Because the historical case experienced notably different hydrodynamics and the bed continued to experience anomalously high rates of erosion and deposition, the bed for the historical case was allowed to evolve for an additional month. The evolved bed was used as the basis for the seasonal model runs, using the bed parameters (with decreased erodibility) given in Table 3.

#### 3.2.2. Fluvial Sediments

Fine-grained sediments were also introduced to the model through the rivers, using the mud and fine mud classes (Figure 1; Table 3). In order to represent the time series of fluvial sediment discharge ($Q_S$), we constructed a rating curve of turbidity versus $Q_R$ for the Coos River using a SSNERR time-series sensor located in the fluvial-estuarine transition zone of the river and iterative model runs to tune the scaling of concentrations (see Section S1). The settling velocities of mud and fine mud were set as 1.0 and 0.1 mm/s, respectively, in order to imitate flocculated and unflocculated mud (see Ralston et al., 2013). The fractions of mud and fine mud assigned to rivers were chosen iteratively until suspended-sediment profiles and time series approximately matched the data gathered during UO surveys and from agency water-quality stations, respectively (Table 3).

### 3.3. Derived Parameters

To evaluate the influence of stratification on vertical mixing and sediment resuspension, we calculate the gradient Richardson ($Ri_g$) number as follows (see Dyer, 1986; Geyer & Smith, 1987; Miles, 1961):

**Table 3**
*Sediment Parameters for Model*

| Parameter | Symbol/units | Coarse sand | Fine sand | Mud (1,2)[a] | Fine mud |
|---|---|---|---|---|---|
| Median grain size | $d_{50}$ (mm) | 0.5 | 0.125 | 0.063 | 0.016 |
| Porosity | $\varphi$ | 0.6 | 0.6 | 0.7 | 0.7 |
| ***Bed evolution run*** | | | | | |
| Settling velocity | $w_s$ (mm/s) | 70 | 10 | 1.0 | 0.1 |
| Erosion rate | $E$ (kg/m$^2$/s) | 1.0e−3 | 1.0e−3 | 1.0e−4 | 1.0e−4 |
| Critical erosion stress | $\tau_e$ (N/m$^2$) | 0.1 | 0.1 | 0.05 | 0.05 |
| Critical deposition stress | $\tau_d$ (N/m$^2$) | 0.0 | 0.0 | 0.05 | 0.05 |
| Initial fraction in bed | $F_0$ | 0.45 | 0.45 | 0.05 | 0.05 |
| ***All other model runs*** | | | | | |
| Settling velocity | -$w_s$ (mm/s) | 100 | 10 | 1.0 | 0.1 |
| Erosion rate | $E$ (kg/m$^2$/s) | 1.0e−4 | 1.0e−4 | 1.0e−4 | 1.0e−4 |
| Critical erosion stress | $\tau_e$ (N/m$^2$) | 3.0 | 1.0 | 0.10 | 0.15 |
| Critical deposition stress | $\tau_d$ (N/m$^2$) | 0.0 | 0.0 | 0.0 | 0.0 |
| Fractions in rivers[b] | – | 0% | 0% | 70% | 30% |
| Fractions in Winchester Creek | – | 0% | 0% | 100% | 0% |

*Note*. All sediments were noncohesive with a density of 2,650 kg/m$^3$.
[a]Mud 1 and 2 had the same properties; Mud 2 was used exclusively as the total suspended load discharged from Winchester Creek. [b]Except Winchester Creek.

$$Ri_g = \frac{-\frac{g}{\rho_0}\frac{\partial \rho}{\partial z}}{\left(\frac{\partial u}{\partial z}\right)^2} \quad (1)$$

where $g$ is the acceleration due to gravity (9.81 m/s$^2$), $\frac{\partial \rho}{\partial z}$ is the density stratification, and $\frac{\partial u}{\partial z}$ is the velocity shear. Fully depth-resolved values were calculated using the velocity and density contrasts between each sigma layer; depth-averaged values of those calculations are reported here. Generally, $Ri_g < 0.25$ represents a threshold below which shear instabilities can occur and turbulence is active, whereas for $Ri_g > 0.25$, stratification tends to damp turbulent motions. In turbulence closure schemes of numerical models, the threshold value of $Ri_g$ that determines how stratification inhibits turbulence can be greater than 0.25, because vertical gradients are not fully resolved (see Umlauf et al., 2003), but $Ri_g$ remains a relevant metric of the dynamical balance.

Sediment transport can be generally described by $uC$ (velocity times sediment concentration). Because $C$ is generally proportional to bed stress, $\tau_b$, and bed stress is proportional to $u^2$, the quantity $u^3$ often scales with sediment transport (Bagnold, 1966; Nidzieko & Ralston, 2012; Winterwerp, 2001). Thus, to evaluate effects of tidal asymmetry on sediment transport, we calculate the cubic ratio of near-bed flood velocities to near-bed ebb velocities $\left(u_{\text{flood}} / u_{\text{ebb}}\right)^3$, using absolute values of each. By calculating the log of the ratio, we can assess whether near-bed sediment transport is expected to be greater on flood tides $\left(\log_{10}\left(\left(u_{\text{flood}} / u_{\text{ebb}}\right)^3\right) > 0\right)$ or ebb tides $\left(\log_{10}\left(\left(u_{\text{flood}} / u_{\text{ebb}}\right)^3\right) < 0\right)$.

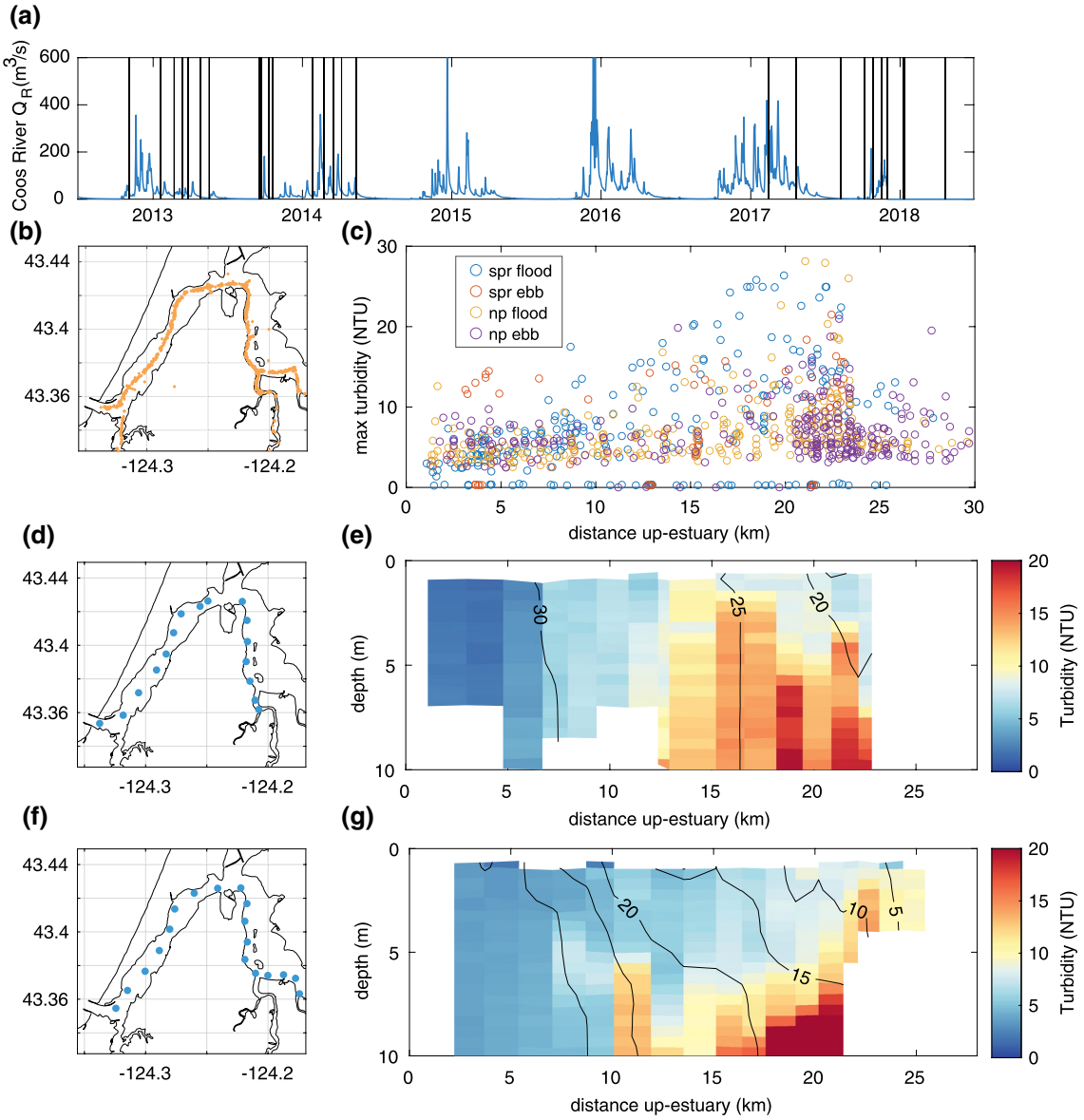


**Figure 4.** Measured salinity and turbidity profiles. (a) Time series of Coos River discharge (sum of East Fork Millicoma, West Fork Millicoma, South Fork Coos, and Marlow Creek data obtained from www.cooswatershed.org). Times of CTD profiles are highlighted. (b) Map of all CTD profiles collected between 2012 and 2018 by UO. (c) Maximum turbidity measured within each vertical profile, shaded by tidal phase and period (spring, neap, flood, and ebb). (d and e) Transect of turbidity (with salinity contours) measured April 27, 2013 (Coos River $Q_R = 9.2$ $m^3$/s, flooding tide). (f and g) Transect of turbidity (with salinity contours) measured February 4, 2017 (Coos River $Q_R = 91.8$ $m^3$/s, flooding tide). CTD, conductivity/temperature/depth.

## 4. Results

River diversion, channel dredging, spoils disposal, and construction in the estuary between 1865 and present have led to an overall increase in suspended-sediment concentrations and sediment retention, as well as re-routing of fine sediment in the upper estuary and formation of an ETM in the navigation channel. Here we describe present-day sediment dynamics and deposits in the estuary, using observations and model results. For the model results, we focus on tidally averaged properties for a 2-day summer period (with low-river discharge, when the estuary tends to be partially mixed) and a 2-day winter period (with high river discharge, when the estuary tends to be stratified; Figure 3). We then contrast these present dynamics to the modeled historical sedimentary processes.

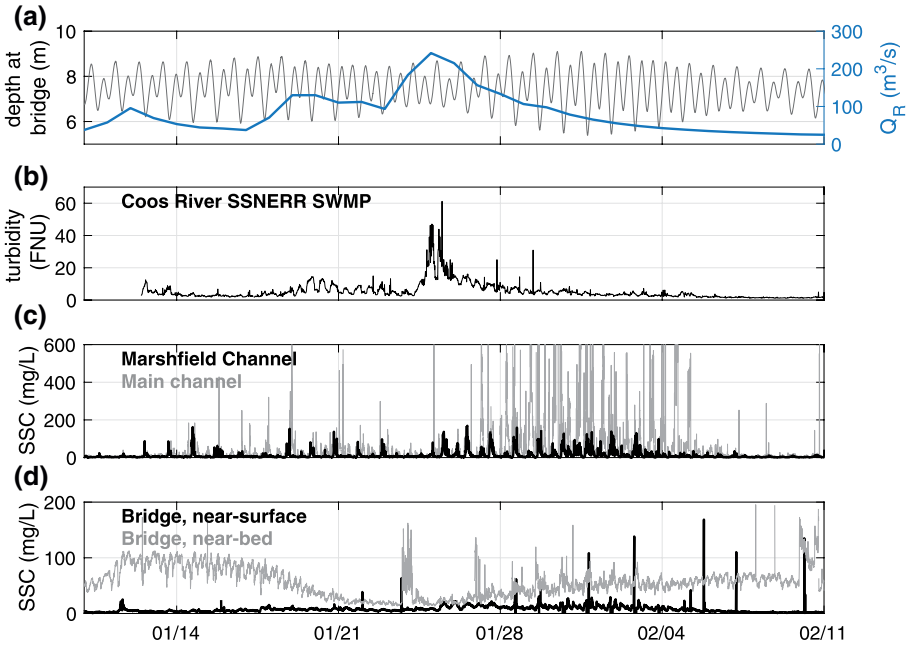


**Figure 5.** River discharge and estuarine suspended-sediment concentrations during a typical winter river discharge event, January–February 2018. (a) Coos River discharge (from www.cooswatershed.org) and water level at the Hwy 101 bridge (Figure 1b). (b) Coos River turbidity from SSNERR SWMP station (Figure 1b). (c) Near-surface and near-bed SSC from fixed sensors mounted at the Hwy 101 Bridge (mooring 3). (d) Near-bed SSC from moored sensors in Marshfield Channel (mooring 1) and the main channel (mooring 2). Mooring locations are provided in Figure 1. SSC, suspended-sediment concentration; SSNERR, South Slough National Estuarine Research Reserve; SWMP, System-Wide Monitoring Program.

### 4.1. Present-Day Sediment Dynamics

The Coos River is the major source of fresh water and sediment to the estuary. At the head of the estuary, much of the Coos River discharge is routed down Marshfield Channel to the navigation channel (Figure 2b), both of which have been dredged and deepened since historical times. In the landward portion of the navigation channel (from ~15 km to 23 km; Figures 2c and 4c), an ETM forms. The maximum turbidities measured in the ETM during low to moderate river discharges (2012–2018) were ~30 NTU (Figure 4c). Depth-maximum turbidities were typically 1.5–2 times greater during flood tides (Figure 4c). Maximum turbidities in the ETM were of a similar order of magnitude (maximum of ~20–30 NTU) for low (~10 m$^3$/s) and moderate (~100 m$^3$/s) river discharges and flood tides (Figures 4d–4g).

Three moorings were deployed in early 2018 (Figure 1b). During a January 2018 river discharge event ($Q_R$ ~200 m$^3$/s; Figure 5), turbidities in the tidal Coos River (SNERR SWMP site, Table 1; Figure 1b) peaked at ~45 FNU. It is worth nothing that NTU, or nephelometric turbidity units, and FNU, formazin turbidity units, are generally both calibrated using the same formazin standards, and will yield the same results for a given standard. In conjunction with this event, SSCs increased to ~40–140 mg/L (varying with tidal phase) at the near-bed mooring 1 in Marshfield Channel, and to ~300 to >600 mg/L in the navigation channel at mooring 2 (Figures 1b and 5c). Farther down-estuary near North Bend (mooring 3), near-bed SSCs were ~10–50 mg/L (though pree-vent SSCs were greater, in conjunction with strong spring tides). In Marshfield Channel, ebb tides were associated with a decrease in salinity from ~15 to 0 and a peak in SSCs. In contrast, SSCs in the main channel generally peaked during flood tides when the salinity was increasing (~15–22; Figure 5c). At the Highway 101 bridge, tidal phasing of peak concentrations was mixed (Figure 5d).

Bed sediments in the modern estuary reflect strong currents in the lower navigation channel, trapping of mud in the upper navigation channel, and slow accumulation of muddy sands in the shallows. Bed sediments sampled between 2009 and 2017 were generally fine to medium sand in the channels, and fine sands to medium silts on shallow intertidal and subtidal flats (Figure 6a). In April 2018, thick unconsolidated mud

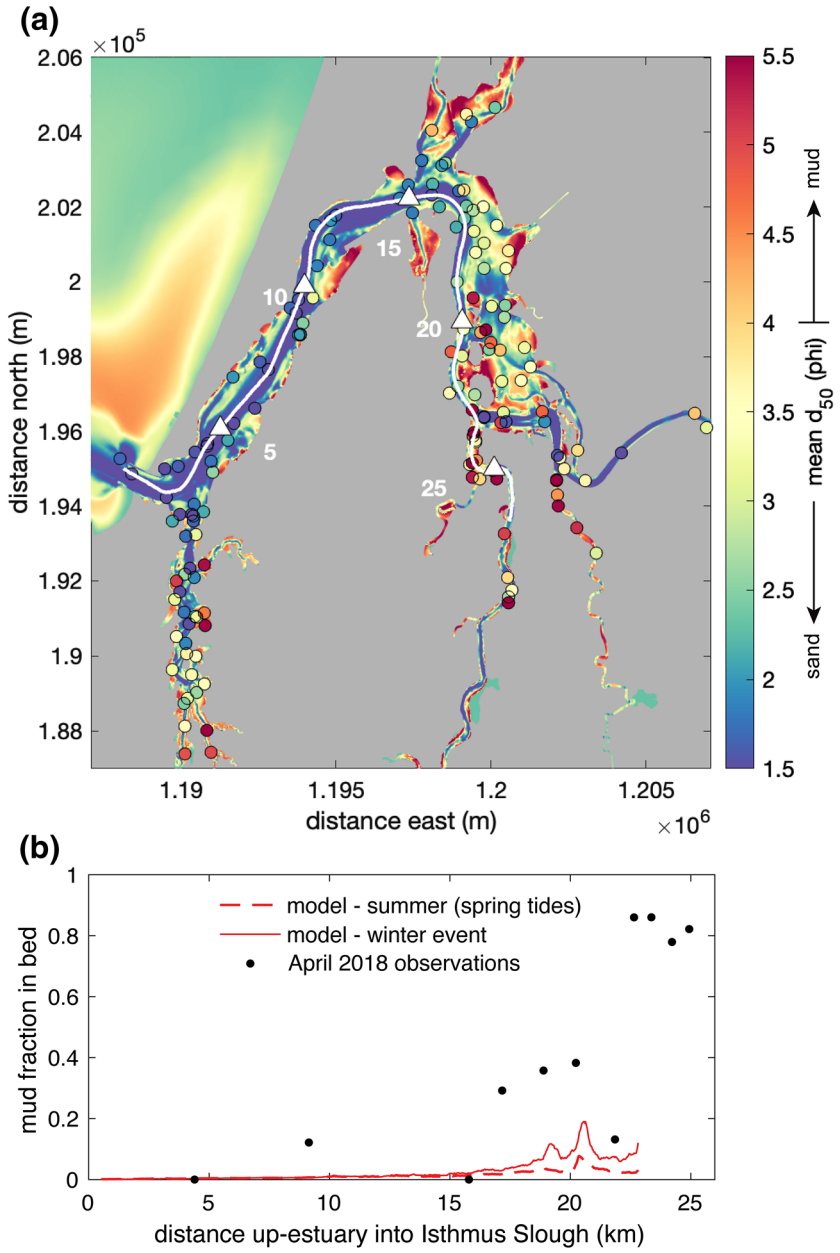


**Figure 6.** Bed sediments. (a) Median seabed grain sizes ($d_{50}$, $\phi$, equivalent to $-\log_2(d_{50}$, mm)) from grab samples and short push cores (circles) and evolved initial model bed for the present bathymetry case (shaded). See Table 2 for parameters used in bed evolution model run. (b) Bed mud fractions in the main channel and Isthmus Slough entrance. Red lines are modeled mud fractions, averaged over the 2-day summer spring tide period and winter 2-day event period (see Figure 3). Black circles are measured mud fractions from an April 2018 grab-sample survey.

with $d_{50}$ of 5.6–6.1 $\phi$ was recovered from grab samples in the upper reaches of the main channel (~20–23 km from the entrance) and in the entrance to Isthmus Slough (Figure 6b). We use the conventional "phi" ($\phi$) size scale here, where $\phi = -\log_2(d_{50}$, mm), and the sand/mud division of 0.063 mm is equal to 4 $\phi$. The evolved bed was used as the initial condition for the seasonal model runs, and qualitatively matched the observed bed sediment sizes, that is, the flats were generally characterized by medium sand to medium silt, and the channels were generally medium sand (Figure 6a).

For the high-discharge event simulated in the model (Figure 3b; peak $Q_R$ = 400 m$^3$/s and peak SSC of ~200 mg/L), near-bed SSCs at moorings 1/2/3 peaked at ~140/60/40 mg/L. In other words, concentrations

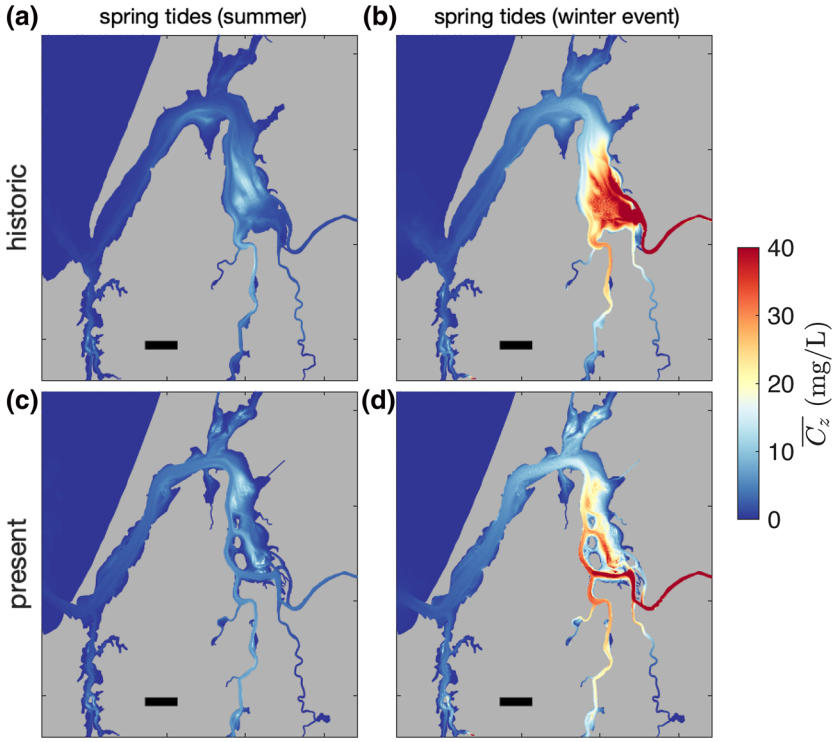


**Figure 7.** Contrasting depth-averaged suspended-sediment concentrations for historical and present cases. (a and b) Tidally averaged $\overline{C_z}$ (over the 2-day periods shown in Figure 3) for the historical bathymetry case. (c and d) Same results for present bathymetry case.

were greatest in Marshfield Channel (and comparable to the values measured during the event in Januaruy 2018) and decreased down-estuary. In the days during and after the event, high SSCs (>20 mg/L) were present during ebb tides between the Coos River and the mooring 3 site (Figures 7d, 8d, and 9h). In the summer, modeled concentrations were low (<10 mg/L) but a weak ETM was present in the same region during spring tides (Figure 9g).

Tidal- and freshwater-modulated hydrodynamics are important for creating the ETM and for dispersing sediment throughout the estuary. Modeled bed stresses, reported in terms of the shear velocity $\left(u^* = \sqrt{\tau_b / \rho}\right)$, are greatest in the channels, and typically exceed 1 cm/s, the nominal threshold of motion for sand, during both summer and winter (low- and high-discharge) periods (Figures 10c–10f, Table 4). Stresses are modulated seasonally, however, by changes in stratification and tidal asymmetry related to changes in freshwater input.

In the summer, near-bed currents in the navigation channel are weakly ebb-dominant and the water column is generally well-mixed (Table 4; Figures 9c and 9e). During winter high-discharge events, the channel becomes weakly flood-dominant and stratified (Figures 9d and 9f), with an average ~26% increase in bed stresses and greater SSCs (Table 4, Figures 9b and 9h). For the tidal flats and side embayments, a similar summer-to-winter transition occurs. Mean summertime bed stresses are ≤1.1 cm/s (Table 4), and the water column is generally well-mixed. The tidal flats and South Slough are ebb-dominant, while smaller side embayments are flood-dominant (Table 4; Figure 11). Winter discharge events increase bed stresses in the embayments and flats by 18%–30%, and the water column becomes more stratified. In contrast to the channel, these shallow regions become more ebb-dominant with the introduction of more fresh water.

In the model, mud deposition primarily occurs during winter events in the Coos River channel, entrances to upper-estuary embayments, the intertidal flats, and the navigation channel—that is, regions proximal to the Coos River source (Figures 12c and 12d). More distal embayments (below 15 km) see limited deposition.

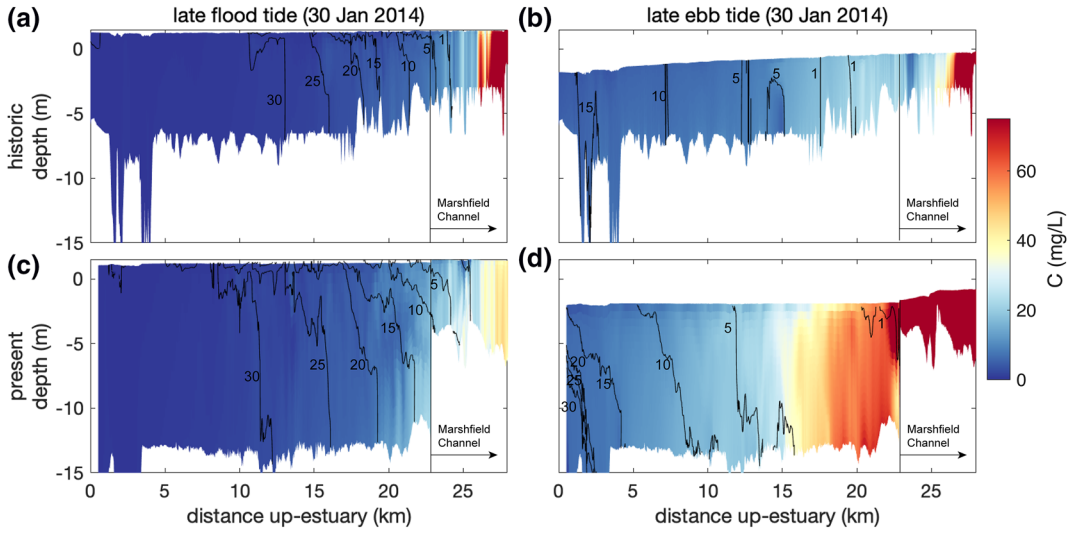


**Figure 8.** Estuarine turbidity maximum during the winter high-discharge event, on 30 Jan 2014, in the main channel thalweg and Marshfield Channel (see Figure 2). (a) Late flood tide, historical case. (b) Late ebb tide, historical case. (c) Late flood tide, present case. (d) Late ebb tide, present case. The entrance to Haynes Inlet is located at approximately 15–16 km upestuary. Salinity contours are shown in black.

The western navigation channel is generally erosional (except on the fringes; Figure 12d). The net sediment retention for 6-week summer and winter periods (represented in Figure 3) is positive in both summer ($2.3 \times 10^4$ kg retained) and winter ($4.7 \times 10^4$ kg retained; Figures 13a and 13f). In the summer, the greatest fraction of total retention occurs on the intertidal flats (Figure 13c), and in winter the greatest fraction of retention occurs in the navigation channel (Figure 13g), though the flats see increased deposition in winter as well (Figure 13h).

### 4.2. Historical Sediment Dynamics

In the historical estuary, hydrodynamics and sediment transport patterns differed because of the direct connection of the Coos River to the tidal flats, and the shallow depths in the primary channel (prior to dredging; Figure 2). The Coos River supplied water and sediment to the eastern edge of the flats, rather than to the navigation channel as in the present case (Figures 7 and 8). Consequently, mean suspended-sediment concentrations on the flats were 60% greater during events than in the present case. Wintertime bed stresses were greater, currents were less ebb dominant, and the flats experienced greater mixing (Table 4, Figure 11). During discharge events, the tidal flats were the dominant location for mud deposition (Figures 12b and 13c).

Beyond the flats, the shallow primary channel received some fine sediment delivered during events (Figures 9j and 12b), but a strong ETM did not form (Figures 7b, 8a, and 8b). The channel was slightly ebb dominant and mixed during discharge events, with ~13% stronger bed stresses than in the present case (Figure 9, Table 4) and depth-averaged suspended-sediment concentrations of <20 mg/L (Figure 9h).

Side embayments (including South Slough) were historically more flood dominant and more well-mixed than in the present case. Exceptions were the tidal flats, which were historically more stratified in summer (Table 4). Depth-averaged suspended-sediment concentrations in shallow regions (flats and embayments) were generally 35%–50% lower than in the present case (Table 4).

Based on the mass of river-derived sediment retained in the estuary over the simulation periods, the modeled historical estuary retained 130% less sediment relative to the present case in summer, and 70% less in winter (Figures 13a and 13f). In summer, the primary channel was net erosional, and minimal deposition occurred in the embayments and South Slough. In winter, the greatest sediment retention occurred on the intertidal flats (Figure 13).

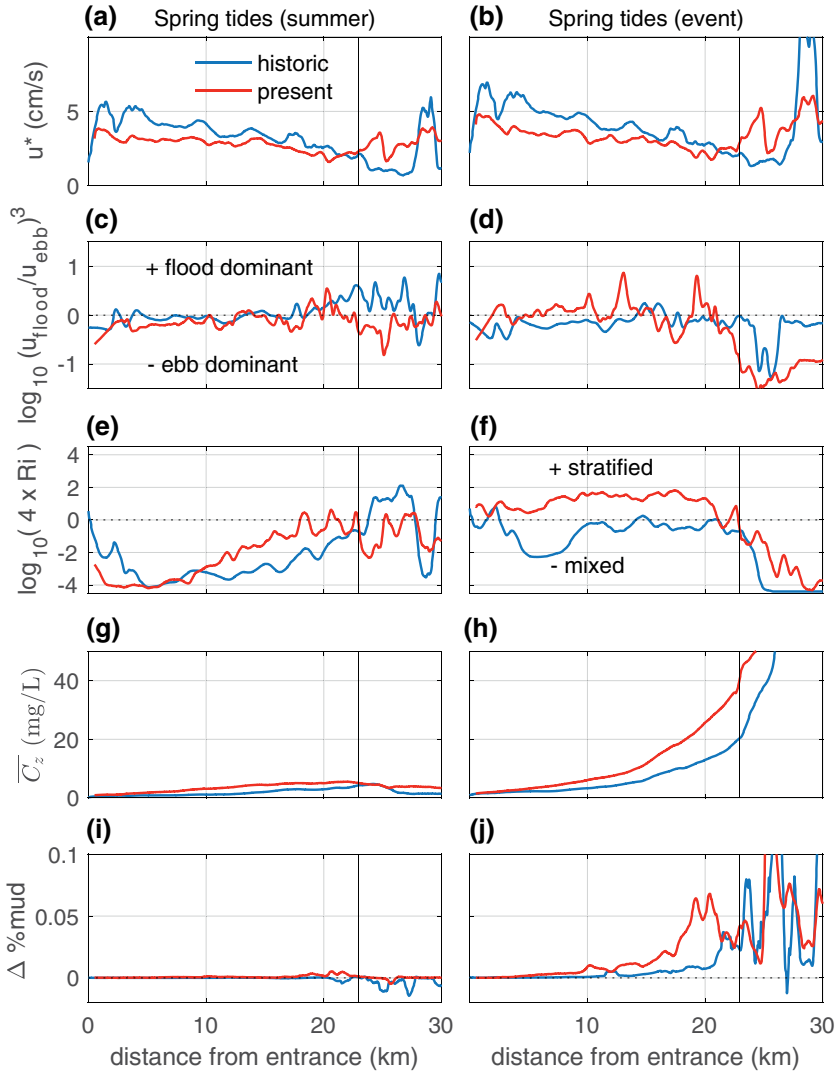


**Figure 9.** Thalweg properties averaged over 2-day time periods (see Figure 3), for historical (blue) and present (red) cases. (a and b) Bed shear velocity. (c and d) Ebb-flood current dominance. (e and f) Bulk $Ri_g$. (g and h) Depth-averaged suspended-sediment concentration. (i and j) Change in percent mud. The vertical line denotes the transition to the shallower Marshfield Channel (see Figure 2 for transect location).

### 4.3. Summary of Key Changes

Changes in hydrodynamics and sediment routing between the historical and modern cases are complex and spatially variable. Since the historical case, the river-estuary connection has been routed away from a shallow, deltaic-style dispersal system and instead into a dredged navigation channel. The adjacent intertidal flats have become more well-mixed in summer, and more stratified in winter, and now retain more sediment. The dredged navigation channel has become more stratified and more ebb-dominant, and has seen a reduction in bed stresses and increase in sediment accumulation.

## 5. Discussion

Channel dredging, intertidal reclamation, and re-routing of the Coos River in the Coos Bay Estuary have altered the hydrodynamics and sediment dynamics of the system, leading to increased tidal amplitudes and increased salinity intrusion (Eidam et al., 2020), and changes in magnitude, spatial patterns, and tidal phasing of bed stresses. Together, these effects have altered how sediment is routed and stored, resulting in

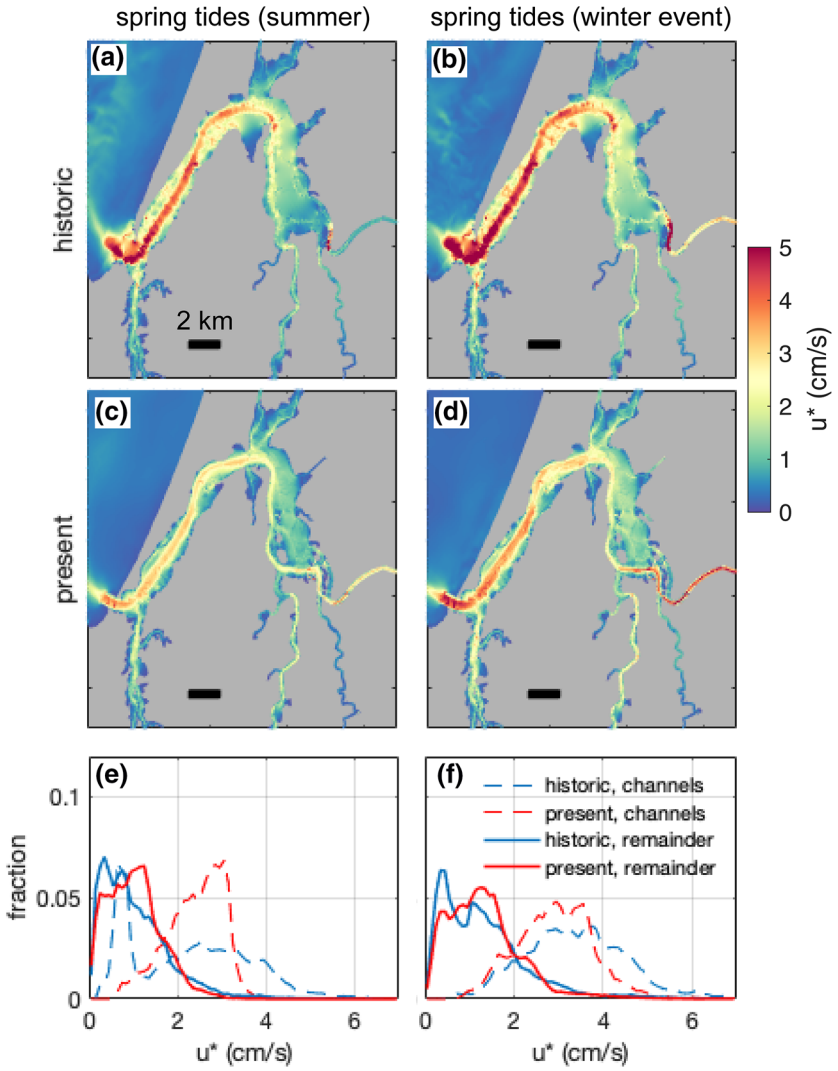


**Figure 10.** Contrasting shear velocities for historical and present cases. (a and b) Tidally averaged $u \times$ magnitude over the 2-day periods highlighted in Figure 3 for the historical bathymetry case. (c and d) Same results for present bathymetry case. (e and f) Histograms of $u^*$, separated into channels (regions with depths >3 m; Figure 1d) and remaining areas.

greater net retention of sediment within the estuary, a stronger and more extensive ETM during high discharge events, and greater sediment trapping in the upper navigation channel. These results highlight the importance of evaluating changes in estuarine hydrodynamics in addition to changes in sediment supply when assessing past sediment histories and attempting to predict future responses to modification, sediment supply, and sea-level change.

### 5.1. Changes in the Point Source of Sediment to the Estuary

The historical configuration of the Coos River-estuary transition can best be described as deltaic intertidal flats (Figure 2a), similar to the Skagit Delta (Ralston et al., 2013). The river discharged through shallow channels across an expansive intertidal area, generating high turbidities (Figure 7c), and a well-mixed water column with ebb-dominant flows during events (Figures 11b and 11d) This type of ebb dominance is expected for tidal flats where salinity gradients are advected onto the flats by flood tides (damping bed stresses), but are then mixed during ebb tides with the influx of river water—creating greater bed stresses and facilitating ebb-directed sediment transport (e.g., Ralston et al., 2013). This ebb dominance serves to

**Table 4**
*Summary of 2-Day Mean Parameters for the Four Subregions Given in Figure 1c, for Summer Spring Tides and Winter Event Period (See Figure 3)*

| | | Channels | | Flats | | Embayments | | South slough | |
|---|---|---|---|---|---|---|---|---|---|
| | | Sum | Win | Sum | Win | Sum | Win | Sum | Win |
| $u^*$ (cm/s) | H | 2.3 | 3.3 | 1.3 | 1.5 | 0.81 | 0.93 | 1.0 | 1.2 |
| | P | 2.3 | 2.9 | 1.1 | 1.3 | 1.0 | 1.3 | 1.1 | 1.4 |
| $\log_{10}\left(u_{\text{flood}} / u_{\text{ebb}}\right)^3$ (+flood/−ebb dominant) | H | 0.16 | −0.13 | 0.08 | −0.27 | 0.27 | 0.28 | 0.08 | 0.21 |
| | P | −0.11 | −0.34 | −0.28 | −0.54 | 0.033 | −0.042 | −0.005 | −0.015 |
| $\log_{10}(4Ri_g)$ (−mixed/+stratified) | H | −2.2 | −1.5 | −2.2 | −1.1 | −0.22 | −0.50 | −0.85 | 0.23 |
| | P | −1.9 | −0.37 | −2.6 | −0.98 | −0.15 | −0.025 | −0.57 | 0.24 |
| Mean depth-averaged SSC (mg/L) | H | 1.7 | 33 | 3.7 | 23 | 1.6 | 5.6 | 0.90 | 2.4 |
| | P | 3.1 | 21 | 4.5 | 14 | 3.1 | 9.8 | 1.5 | 3.7 |

Abbreviations: H, historic; P, present; SSC, suspended-sediment concentration.

transport sediment seaward, but in the Coos Bay case, the expansive intertidal flats served as a relatively effective sink (Figure 12b; Video S1), preventing much of the fine-grained sediment from reaching the primary channel of the estuary (Figure 7b vs. Figure 7d)—a trapping process which helped limit the development of a primary-channel ETM (Figures 7 and 8).

As expected, ebb dominance was greatest during wintertime high-discharge events (Figure 11d), when $Ri_g$ values were <0.25 (Figure 11b). During summer periods, $Ri_g$ values on the flats reflected greater salinities

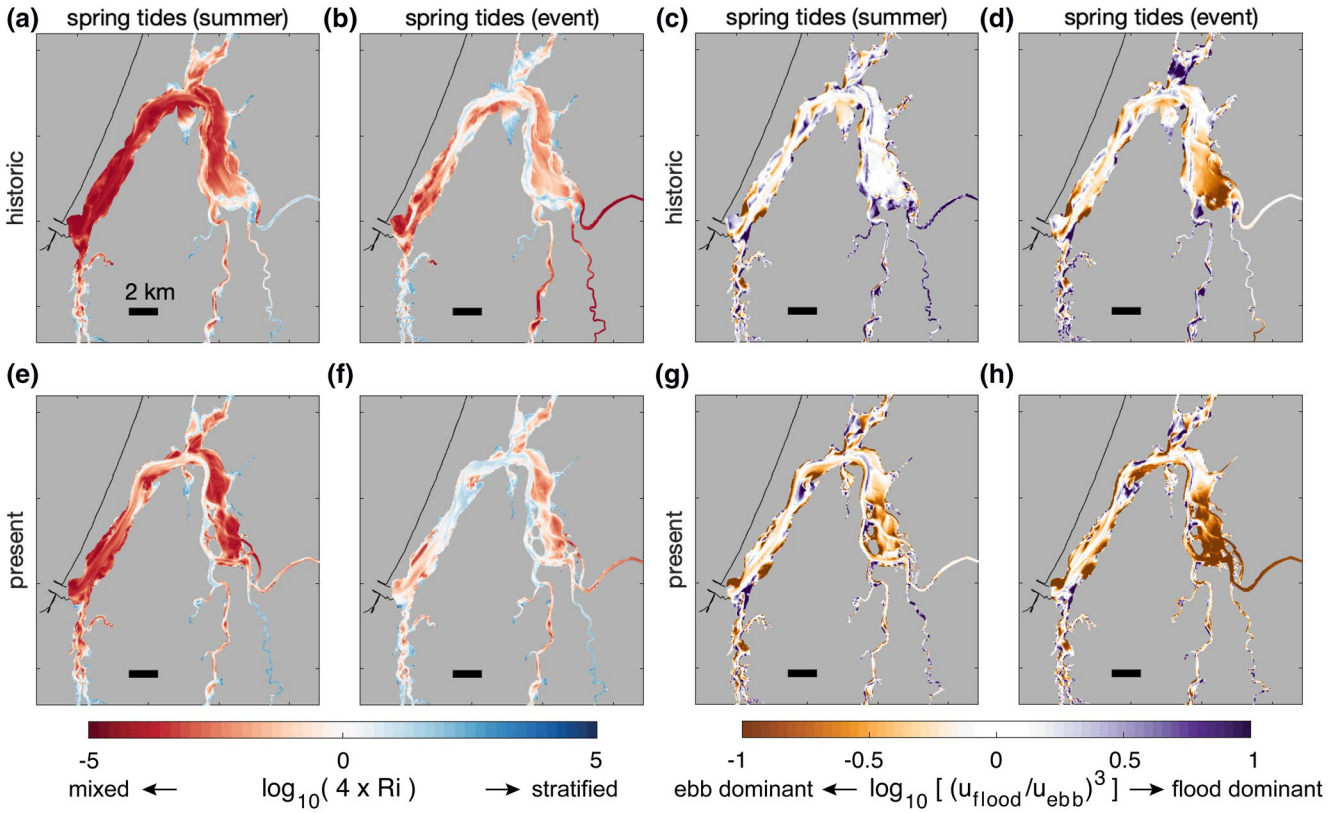


**Figure 11.** (a, b, e, f) Contrasting stratification for historical and present cases, expressed as $\log_{10}(4 \times Ri_g)$. Red colors indicate greater mixing (generally leading to greater bed stress) and blue colors indicate greater stratification. $Ri_g = 0.25$ is represented by $\log_{10}(4 \times Ri_g) = 0$. (c, d, g, h) Ratio of flood to ebb currents within the estuary, expressed in terms of $\log_{10}(u_{\text{flood}}/u_{\text{ebb}})^3$. Negative (orange) values denote ebb-dominant currents, and positive values (purple) denote flood-dominant currents.

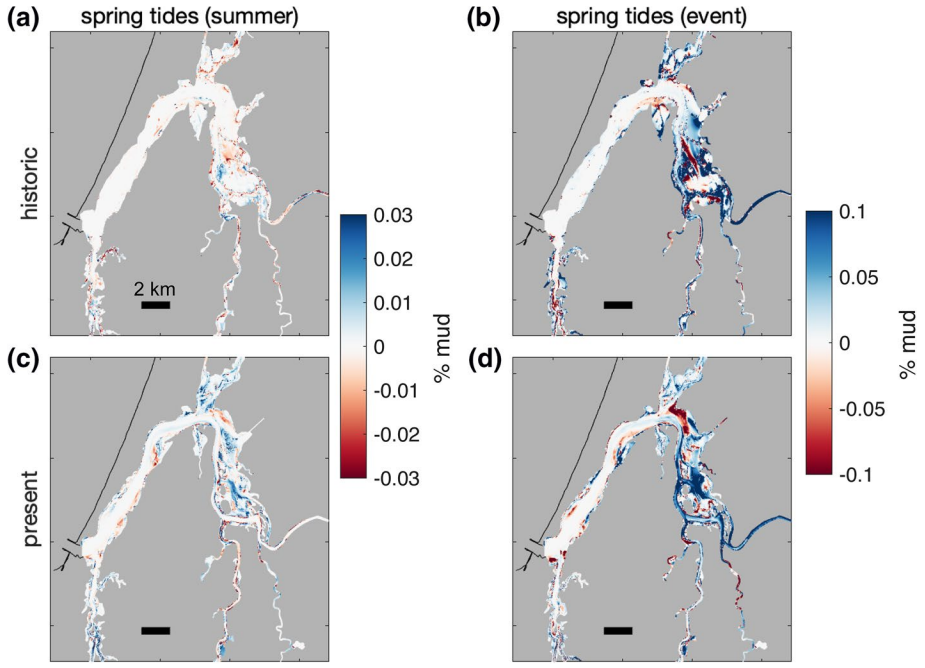


**Figure 12.** Changes in percent mud for the 2-day periods given in Figure 3. (a and b) Change in percent mud for the historical bathymetry case. (c and d) Same results for present bathymetry case.

and slightly stronger salinity gradients, and tidal velocities were relatively symmetric in terms of mean magnitude between flood and ebb (Figure 11c). Sediments were gradually winnowed from the flats during summer (Figures 12a, 12b, and 13c), likely by gradual diffusive transfer between shallow regions that had received fresh winter mud and the coarser-grained channel (see Mariotti & Fagherazzi, 2012).

In the present case, the Coos River is routed down Marshfield Channel (a dredged channel), past intertidal regions that have been largely reclaimed by spoils disposal (Figure 2b). Marshfield Channel is ebb dominant

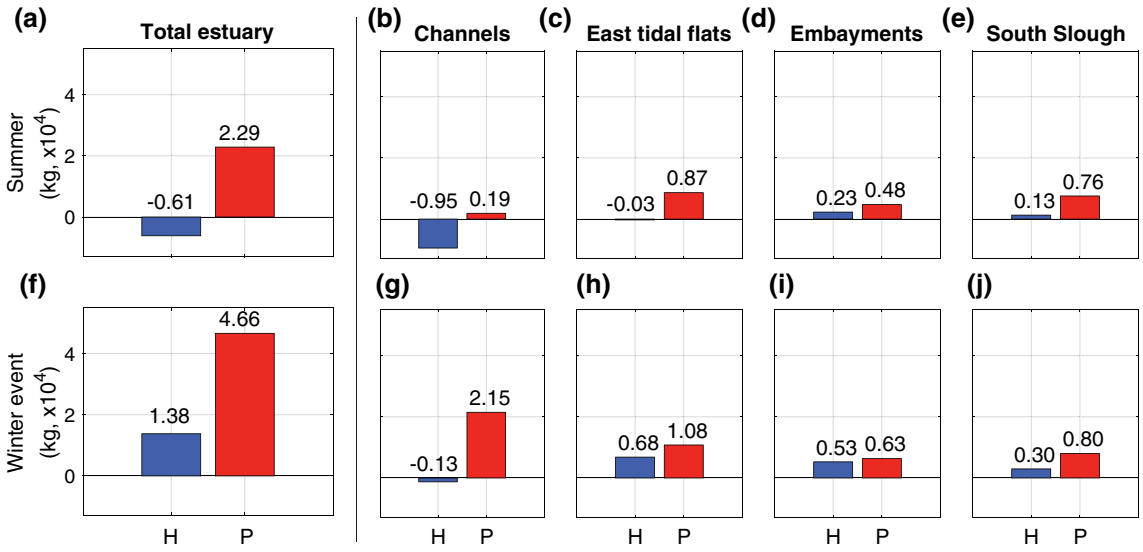


**Figure 13.** Sediment retention and export from estuary during the 6-week period highlighted in Figure 3. H = historical and P = present case. (a–e) Summer case. (f–j) Winter "event" case. Positive values mean sediment was accumulated in the estuary during the 6-week period, and negative values indicate a net export of sediment. The first column represents the total estuary, and columns to the right indicate a breakdown of retention and export by areas (see Figure 1c).

in summer and winter (Figures 9c, 9d, and 11h) with $u^*$>1 cm/s (Figures 9a and 9b), and thus serves as an effective conduit for fluvial delivery of sediment to the main channel (below 23 km)—as noted in the mooring data from 2018 (Figure 5c). This geometry represents a more channelized river-estuary transition than the historical case (and common to many larger estuaries), and helps facilitate formation of an ETM in the navigation channel (Section 5.2, Figure 4).

### 5.2. Changes in Thalweg Hydrodynamics and ETM Dynamics

Historically, the thalweg was shallower and characterized by higher bed stresses, weaker tidal asymmetry, and greater mixing than in the present case (Figures 2a, 9a–f, 10a, and 10b; Table 4), and was generally erosional (Figures 9a, 9b, and 13b; Table 4). Channel deepening has altered the hydrodynamics and effectively created a sediment sink, landward of ~15 km (Figures 2b and 12d). In estuaries, channel deepening typically causes reduced hydraulic drag, tidal amplification, increased salinity intrusion, and increased estuarine circulation—processes which serve to increase landward transport of sediment and increased convergence of sediment at the freshwater-saltwater transition (e.g., Burchard et al., 2018; de Jonge et al., 2014; Geyer, 1993; van Maren, van Kessel, et al., 2015; Winterwerp et al., 2013). In Coos Bay, an almost doubling of the channel depth (Figure 2c) has led to a 33% increase in tidal amplitude, increased salinity intrusion, and increased exchange flow (Eidam et al., 2020), as well as increased stratification (Figure 9f).

The increased channel depth has impacted sediment transport through decreased bed stress (Figures 9a, 9b, and 10). This effect is related to decreased current magnitude (Eidam et al., 2020), increased near-bed flood dominance of currents (Figure 9d), and increased stratification in the thalweg (~0-21 km; Figure 9f)—effects common in deepened channels (see Geyer, 1993). The resulting reduction in bed stress allows for greater sediment-retention potential due to reduced transport energy. Furthermore, while the channel thalweg has become slightly more ebb-dominant during summer periods when mixing dominates (Figure 9c), the system has become more flood-dominant (~0-21 km) during winter periods when stratification increases (Figure 9d) and fluvial sediment loads are high. This shift from ebb-dominant to flood-dominant channel stresses during winter periods (Figure 9d) facilitates trapping of sediment in the main channel, which is evident in the unconsolidated mud recovered from the upper channel in April 2018 (Figure 6b) and need for ongoing maintenance dredging by the Army Corps (e.g., Briner, 2009; USACE, 2015). This change is expected from a hydrodynamics perspective (increased exchange flow) and from a geologic perspective (increased accommodation space in a channel deepened by ~4 m, relative to a tidal amplitude increase of ~2 m, Figure 2c and Burchard et al., 2018; Davis & Dalrymple, 2011; Eidam et al., 2020; Meade, 1969; Slagle et al., 2006).

In addition to promoting sediment trapping and more direct delivery down Marshfield Channel, the altered bathymetry of the dredged navigational channel has promoted the formation of an ETM that was not present in the historical case (Figures 7b, 7d, 8, 9g and 9h). This feature was observed during the moderate discharge event in January 2018 (Figure 5), when near-bed sensors recorded SSCs of >200 mg/L in the main channel (mooring 2) and >50 mg/L near North Bend (mooring 3, Figure 1b). An ETM was also observed in multiple thalweg surveys between 2012 and 2018 (Figure 4). Modeled SSCs were not as strong as those measured (Figure 9l), likely because the model did not have time to develop a sufficiently large pool of bottom sediment which could then feed the ETM through resuspension, as has been observed in other estuaries (e.g., Burchard et al., 2018; Geyer & Ralston, 2018). The existence of a muddy reservoir of sediment in upper Coos Bay is likely, however, based on modeled patterns of deposition during events (Figures 9j and 12d), program of frequent maintenance dredging (Briner, 2009; USACE, 2015), and unconsolidated muddy sediments recovered from the upper navigation channel in April 2018 (Figure 6b), as noted above. Given a longer run time of several years, the model might develop this muddy reservoir and greater SSC in the ETM, based on the convergence of sediment in the channel observed for the brief winter runs (Figure 12d).

### 5.3. Sediment Delivery to Shallow Regions

A key consequence of dredging and development of an ETM is altered routing of sediments to the tidal flats and some side embayments. While the diversion of the Coos River into the navigation channel has reduced the delivery of sediments to the southern flats (Figures 7b and 7d), the ETM formed in the main

channel now serves as a source of sediment along the western edge of the flats, owing to lateral transfer. Lateral transfer of sediment from channels to flats occurs in many estuaries, owing to positive gradients of sediment concentrations, and lateral circulation (e.g., Fugate et al., 2007; Mariotti & Fagherazzi, 2012; McSweeney et al., 2016). During discharge events, suspended sediments sourced from the main channel are advected onto the northern flats in the present case during flood tides (Video S1)—thus, even though fluvial mud may initially bypass the flats, it may be re-imported farther north, fed by the primary channel ETM, and thus allow an overall increase in storage on the shallow flats.

A similar effect of lateral transfer has likely been intensified compared to the historical conditions for side embayments like Haynes Inlet, which now sees greater SSCs during events (Figure 7d). The present-day ETM extends to the Haynes entrance at ~15 km during events (Figure 8d), and sediment suspended near the top of the water column can be advected into the embayment, where flood-dominant currents and stratification in the shallows promote trapping (Figures 11f and 11h). This style of supply to embayments was observed in the Connecticut Estuary, both because the ETM was located near an embayment entrance, and salinity gradients and stratification were conducive to sediment import and trapping within the side basin (Yellen et al., 2017). In Haynes, the modeled increase in trapping is supported by a record of increased sediment accumulation from upper Haynes Inlet, where sedimentation rates increased from ~0.5 cm/yr to >1 cm/yr ~50 years ago (Johnson et al., 2019), approximately 20 years after Marshfield Channel was first dredged (Eidam et al., 2020).

Overall, side embayments experienced 20%–480% more retention in the present case than historical case (Figures 13d and 13i). For embayments in the upper estuary, this retention is likely related to increased sediment supply from the Marshfield Channel and/or the primary navigation channel. Hydrodynamics also play a role; bed stresses have increased, but the embayments remain generally flood dominant (or only very weakly ebb dominant during events; Table 4), allowing resuspended sediment to remain trapped.

### 5.4. Implications

Many larger, more turbid estuaries have been modeled using depth- or width-averaged models, in order to assess the intensification of an ETM post-dredging, and in some cases the development of secondary ETMs (e.g., Grasso & Le Hir, 2019; van Maren, Winterwerp, et al., 2015; van Rijn & Grasmeijer, 2018). Typically, these estuaries experience an upstream migration and intensification of the ETM due to amplification of tidal currents and estuarine circulation, and greater salt-wedge propagation. Coos Bay, modeled here using a high-resolution, 3D hydrodynamic model (Conroy et al., 2020), provides a view into the formation of an ETM in a system which historically had a deltaic style river outlet (rather than a classic, simple, funnel-shaped, river-estuary transition) and complex geometry related to regional tectonics. In this system, dredging diverted water and sediment from the shallow flats into a deep navigation channel, which (aided by a change in the bathymetry by dredging) allowed for the formation of a more classic ETM. This diversion and dredging also created new accommodation space and hydrodynamics conducive to sediment storage, creating a negative feedback for dredging. The evolution of this new ETM has also offset the diversion of the river away from the intertidal flats, by providing a "new" source of sediment to the flats from the navigation channel itself (Video S1)—as well as a source of sediment to nearby side embayments.

Dredging has led to reduced bed stresses in many parts of the estuary (Figure 10), but suspended-sediment concentrations have generally increased—likely due to the stronger ETM and pool of fine sediment now present in the main channel. In South Slough, bed stresses have generally increased, together with sediment concentrations—likely because of increased tidal amplitudes, increased salt wedge propagation (see Eidam et al., 2020), and reduced stratification on the seaward side of the salt wedge in summer (and on the landward side during events).

Changes in sediment concentrations and bed properties are of relevance to local habitat restoration efforts for eelgrass and oysters (Groth & Rumrill, 2009; Thom et al., 2003). In these simulations, differences between the historical and modern conditions are highly variable throughout the system. For example, shallow mid-estuary sites near the airport and in Haynes Inlet have transitioned from dominantly sandy to dominantly muddy substrates, while sites in the lower estuary (South Slough) and upper estuary (entrances to Catching and Coalbank sloughs) have seen the opposite trend. Meanwhile, some habitat sites have seen

effectively no change. Suspended-sediment concentrations have generally increased, but still remain relatively low (<50 mg/L), when averaged over monthly timescales.

Many attempts to model changing sediment concentrations in estuaries have focused on understanding the problematic transition to "hyperturbid" conditions, that is, sediment concentrations of many grams per liter (e.g., Dijkstra, Schuttelaars, Brouwer, & Schramkowski, 2019b; van Maren, Winterwerp, et al., 2015; Winterwerp, 2011). While Coos Bay provides an example of ETM development in a system where the river input transitioned from deltaic to channelized, transition to a hyperturbid state seems unlikely. The "characteristic" SSC of an estuary is thought to be a function of its tidal amplitude and length, and a typical SSC of ~30 mg/L for Coos Bay fits well in this framework as predicted by Uncles et al. (2002) and Uncles and Smith (2005). Based on the ~33% increase in tidal amplitude over the past 150 years (Eidam et al., 2020), SSCs in Coos Bay would be predicted to double, remaining less than ~100 mg/L (see Uncles & Smith, 2005). The work here, based on a hydrodynamic model indicating a doubling of estuarine exchange flow, suggests that concentrations have in fact doubled (Figures 9j–9l). This effect is likely understated due to the development of a muddy pool of sediment as described above (see also Figure 5), but the persistence of relatively low SSCs despite 150 years of modification suggests that Coos Bay is not likely to develop extremely turbid conditions in the near future.

Local managers are also interested in the effects of sea-level rise and changing sediment supplies on estuarine habitats and ecosystems. While neither of these effects is modeled here, it is interesting to note that for the same sea level and sediment loads, total estuarine sediment storage and mean suspended-sediment concentrations both increased over 150 years simply due to hydrodynamic changes induced by dredging and other modifications. Sea-level rise should in theory further increase retention in the estuary, by increasing accommodation space (though concurrent changes in hydrodynamics may confound this effect). An increase in watershed sediment loads (which may have been affected by logging, an industry important through the 1980s; Johnson et al., 2019; Robbins, 1984) could amplify the effects of increased sediment concentrations already caused by hydrodynamic changes. It should also be noted that storage may be overpredicted and SSC may be underpredicted in the model, due to wind and wave effects (see Baptist et al., 2019; Green & Coco, 2014; Schulz et al., 2018), which were not modeled here. Future work addressing wave resuspension on the flats, and tidal flat records of sediment delivery changes through time, would help validate past patterns of changing storage.

## 6. Conclusion

Modifications to channel depths and shallow areas in the past 150 years have altered water and sediment dynamics in Coos Bay. Based on results from a detailed hydrodynamic model, deepening of the primary channel has increased the tidal amplitude, exchange flow, and salinity intrusion length (Eidam et al., 2020). In addition, reconfiguration of the primary river mouth has re-routed water and sediment directly into that dredged channel, whereas previously it discharged onto deltaic tidal flats. These changes have had six key impacts on sediment routing and storage in the system:

- Sediment is now diverted away from the intertidal flats and toward the deepened navigation channel, creating an estuary with a more classic river-channel transition rather than river-deltaic flats transition. This change has been facilitated by re-routing of the river down Marshfield Channel, which acts as an efficient conduit due to dredging and adjacent intertidal reclamation.
- Direct delivery to the channel combined with hydrodynamic effects of channel deepening (greater stratification, reduced bed stress, greater exchange flow, and more flood-dominant currents during high discharge events) have led to the development of a bathymetric estuarine turbidity maximum and increased mud deposition in the estuary during discharge events.
- Despite the diversion of river sediment inputs away from the intertidal flats, the intertidal flats now receive more sediment via lateral transport from the main channel ETM, and have greater net storage than in the past—even without accounting for increased accommodation due to sea-level rise.
- Embayments near the new ETM (Haynes Inlet) retain more sediment, given greater bed stresses, generally flood-dominant currents, and a greater supply of sediment from the ETM. South Slough also retains more sediment, though it is located farther from the primary channel ETM.

- Overall, suspended-sediment concentrations have generally increased by a factor of two for the modeled cases, though actual changes over the past century would also depend on changing sediment loads from the watershed, as well as the long-term (multiyear) accumulation of muddy sediment in the main channel (as was observed in April 2018).
- The modeled estuary retains more sediment in the modern than historical case, without accounting for increased accommodation from sea-level rise or changing sediment loads related to land-use change.

These results highlight the need to consider hydrodynamic impacts due to dredging when evaluating changes in sedimentation rates in an estuary. In the absence of other external shifts (e.g., sea-level rise and land-use change), dredging can intensify sediment concentrations and retention—and in estuaries with complex geometries like Coos Bay, these effects can have spatially distinct impacts on the transport pathways and changes in bed sediment characteristics among channels, shallow flats, and side embayments.

## Data Availability Statement

Model computations were performed on the University of Oregon high-performance computer Talapas. Data are archived at https://accession.nodc.noaa.gov/0210797.

**Acknowledgments**
This work was sponsored by the National Estuarine Research Reserve System Science Collaborative, which supports collaborative research that addresses coastal management problems important to the reserves. The Science Collaborative is funded by the National Oceanic and Atmospheric Administration and managed by the University of Michigan Water Center (NAI4NOS4190145). We thank the staff at the South Slough National Estuarine Research Reserve, OIMB, the Coos Watershed Association, and CTCLUSI for their field, logistical, and data support. We also thank Kira Bartlett for assistance with the historic bathymetry digitization. We appreciate comments from two reviewers and Associate Editor Chris Sherwood, which helped improve the study.

## References

Bagnold, R. A. (1966). *An approach to the sediment transport problem* (General Physics Geological Survey Professional Paper 422–I, pp. 231–291). Washington, DC: US Government Printing Office.
Baker, C. A. (1978). *A study of estuarine sedimentation in South Slough*. Coos Bay, OR: Portland State University.
Baptista, A. M. (1989). *Salinity in Coos Bay, Oregon: Review of historical data (1930–1989)* (Report ESE–89–001). Portland, OR: U.S. Army Engineer District.
Baptist, M. J., Gerkema, T., Van Prooijen, B. C., Van Maren, D. S., Van Regteren, M., Schulz, K., et al. (2019). Beneficial use of dredged sediment to enhance salt marsh development by applying a 'Mud Motor'. *Ecological Engineering*, *127*, 312–323.
Barbier, E. B., Hacker, S. D., Kennedy, C., Koch, E. W., Stier, A. C., & Silliman, B. R. (2011). The value of estuarine and coastal ecosystem services. *Ecological Monographs*, *81*(2), 169–193. http://doi.org/10.1890/10-1510.1
Beaulieu, J. D., & Hughes, P. W. (1975). Environmental geology of western Coos and Douglas counties, Oregon (Bulletin 87). Portland, OR: State of Oregon, Department of Geology and Mineral Industries.
Blott, S. J., Pye, K., Van der Wal, D., & Neal, A. (2006). Long-term morphological change and its causes in the Mersey Estuary, NW England. *Geomorphology*, *81*(1–2), 185–206.
Borde, A. B., Thom, R. M., Rumrill, S., & Miller, L. M. (2003). Geospatial habitat change analysis in Pacific Northwest coastal estuaries. *Estuaries*, *26*(4), 1104–1116. http://doi.org/10.1007/BF02803367
Briner, W. (2009). *Coos Bay sediment quality evaluation report* (Tech. Rev CENWP-EC-HR). Portland, OR: US Army Corps of Engineers.
Brophy, L. (2017). *Indirect assessment of west coast USA tidal wetland loss. File geodatabase feature class, Pacific Marine and Estuarine Fish Habitat Partnership*. Retrieved from https://www.pacificfishhabitat.org/data/tidal-wetlands-loss-assessment/
Burchard, H., Schuttelaars, H. M., & Ralston, D. K. (2018). Sediment trapping in estuaries. *Annual Review of Marine Science*, *10*(1), 371–395. http://doi.org/10.1146/annurev-marine-010816-060535
Caldera, M. (1995). *South Slough Adventures: Life on a Southern Oregon Estuary*. Coos Bay, OR: Friends of South Slough, South Coast Printing Company.
Chant, R. J., Sommerfield, C. K., & Talke, S. A. (2018). Impact of channel deepening on tidal and gravitational circulation in a highly engineered estuarine basin. *Estuaries and Coasts*, *41*(6), 1587–1600.
Chen, C., Liu, H., & Beardsley, R. C. (2003). An unstructured grid, finite-volume, three-dimensional, primitive equations ocean model: application to coastal ocean and estuaries. *Journal of Physical Oceanography*, *20*, 159–186.
Conroy, T., Sutherland, D. A., & Ralston, D. K. (2020). Estuarine exchange flow variability in a seasonal, segmented estuary. *Journal of Physical Oceanography*, *50*, 505–613.
Davis, R. A., Jr, & Dalrymple, R. W. (Eds.). (2011). *Principles of tidal sedimentology*, New York, NY: Springer Science & Business Media.
de Jonge, V. N., Schuttelaars, H. M., van Beusekom, J. E., Talke, S. A., & de Swart, H. E. (2014). The influence of channel deepening on estuarine turbidity levels and dynamics, as exemplified by the Ems estuary. *Estuarine, Coastal and Shelf Science*, *139*, 46–59.
Dicken, S. N., Hanneson, B., & Johannessen, C. L. (1961). *Some recent physical changes of the Oregon coast* (p. 151). Eugene, OR: Department of Geography, University of Oregon.
Dijkstra, Y. M., Schuttelaars, H. M., & Schramkowski, G. P. (2019a). A regime shift from low to high sediment concentrations in a tide-dominated estuary. *Geophysical Research Letters*, *46*(8), 4338–4345. https://doi.org/10.1029/2019GL082302
Dijkstra, Y. M., Schuttelaars, H. M., Schramkowski, G. P., & Brouwer, R. L. (2019b). Modeling the transition to high sediment concentrations as a response to channel deepening in the Ems River Estuary. *Journal of Geophysical Research: Oceans*, *124*(3), 1578–1594. https://doi.org/10.1029/2018JC014367
Dyer, K. (1986). *Coastal and estuarine sediment dynamics* (p. 358). Chichester, UK: John Wiley and Sons.
Eidam, E. F., Sutherland, D. A., Ralston, D. K., Dye, B., Conroy, T., Schmitt, J., et al. (2020). Impacts of 150 years of shoreline and bathymetric change in the Coos Estuary, Oregon, USA. *Estuaries and Coasts*, 1–19.
Familkhalili, R., & Talke, S. A. (2016). The effect of channel deepening on tides and storm surge: A case study of Wilmington, NC. *Geophysical Research Letters*, *43*, 1–10. http://doi.org/10.1002/2016GL06949410.1002/(ISSN)1944-8007
Fugate, D. C., Friedrichs, C. T., & Sanford, L. P. (2007). Lateral dynamics and associated transport of sediment in the upper reaches of a partially mixed estuary, Chesapeake Bay, USA. *Continental Shelf Research*, *27*(5), 679–698.

Geyer, W. R. (1993). The importance of suppression of turbulence by stratification on the estuarine turbidity maximum. *Estuaries*, *16*(1), 113–125.
Geyer, W. R., & Ralston, D. K. (2018). A mobile pool of contaminated sediment in the Penobscot Estuary, Maine, USA. *Science of the Total Environment*, *612*, 694–707.
Geyer, W. R., & Smith, J. D. (1987). Shear instability in a highly stratified estuary. *Journal of Physical Oceanography*, *17*(10), 1668–1679.
Grasso, F., & Le Hir, P. (2019). Influence of morphological changes on suspended sediment dynamics in a macrotidal estuary: diachronic analysis in the Seine Estuary (France) from 1960 to 2010. *Ocean Dynamics*, *69*(1), 83–100.
Green, M. O., & Coco, G. (2014). Review of wave-driven sediment resuspension and transport in estuaries. *Reviews of Geophysics*, *52*(1), 77–117. https://doi.org/10.1002/2013RG000437
Groth, S., & Rumrill, S. (2009). History of Olympia oysters (Ostrea lurida carpenter 1864) in Oregon estuaries, and a description of recovering populations in Coos Bay. *Journal of Shellfish Research*, *28*(1), 51–58. http://doi.org/10.2983/035.028.0111
Guerry, A. D., Ruckelshaus, M. H., Arkema, K. K., Bernhardt, J. R., Guannel, G., Kim, C.-K., et al. (2012). Modeling benefits from nature: using ecosystem services to inform coastal and marine spatial planning. *International Journal of Biodiversity Science, Ecosystem Services & Management*, *8*, 107–121. https://doi.org/10.1080/21513732.2011.647835
Hickey, B. M., & Banas, N. S. (2003). Oceanography of the US Pacific Northwest coastal ocean and estuaries with application to coastal ecology. *Estuaries*, *26*(4), 1010–1031.
Hoffnagle, J., & Olson, R. (1974). *Salt marshes of the Coos Bay Estuary*. Charleston, SC: Oregon Institute of Marine Biology.
Ivy, D. (2015). A brief overview of the Coos Bay area's economic and cultural history. In C. E. Cornu, & J. Souder (Eds.), *Communities, lands & waterways data source*. Coos Bay, OR: Partnership for Coastal Watersheds, South Slough National Estuarine Research Reserve, and Coos Watershed Association.
Jay, D. A., Talke, S. A., Hudson, A., & Twardowski, M. (2015). Estuarine turbidity maxima revisited: Instrumental approaches, remote sensing, modeling studies, and new directions. *Developments in Sedimentology*, *68*, 49–109.
Johnson, G. M., Sutherland, D. A., Roering, J. J., Mathabane, N., & Gavin, D. G. (2019). Estuarine dissolved oxygen history inferred from sedimentary trace metal and organic matter preservation. *Estuaries and Coasts*, *42*(5), 1211–1225.
Komar, P. D., Allan, J. C., & Ruggiero, P. (2011). Sea level variations along the US Pacific Northwest coast: Tectonic and climate controls. *Journal of Coastal Research*, *27*(5), 808–823.
Lane, A. (2004). Bathymetric evolution of the Mersey Estuary, UK, 1906–1997: Causes and effects. Estuarine. *Coastal and Shelf Science*, *59*(2), 249–263. http://doi.org/10.1016/j.ecss.2003.09.003
Lotze, H. K. (2010). Historical reconstruction of human-induced changes in U.S. Estuaries. In R. N. Gibson, R. J. A Atkinson & J. D. M. Gordon (Eds.), Oceanography and marine biology—An annual review (2nd ed., Vol. 20103650, pp. 267–338). New York, NY: CRC Press. http://doi.org/10.1201/ebk1439821169-c5
Lotze, H. K., Lenihan, H. S., Bourque, B. J., Bradbury, R. H., Cooke, R. G., Kay, M. C., et al. (2006). Depletion, degradation, and recovery potential of estuaries and coastal seas. *Science*, *312*(5781), 1806–1809.
Mariotti, G., & Fagherazzi, S. (2012). Channels-tidal flat sediment exchange: The channel spillover mechanism. *Journal of Geophysical Research*, *117*(C3). https://doi.org/10.1029/2011JC007378
McSweeney, J. M., Chant, R. J., & Sommerfield, C. K. (2016). Lateral variability of sediment transport in the Delaware Estuary. *Journal of Geophysical Research: Oceans*, *121*(1), 725–744. https://doi.org/10.1002/2015JC010974
Meade, R. H. (1969). Landward transport of bottom sediments in estuaries of the Atlantic coastal plain. *Journal of Sedimentary Research*, *39*(1), 222–234.
Miles, J. W. (1961). On the stability of heterogeneous shear flows. *Journal of Fluid Mechanics*, *10*(4), 496–508.
Nichols, M. M., & Howard-Strobel, M. M. (1991). Evolution of an Urban Estuarine Harbor: Norfolk, Virginia. *Journal of Coastal Research*, *7*(3), 745–757.
Nidzieko, N. J., & Ralston, D. K. (2012). Tidal asymmetry and velocity skew over tidal flats and shallow channels within a macrotidal river delta. *Journal of Geophysical Research*, *117*(C3). https://doi.org/10.1029/2011JC007384
Nnafie, A., de Swart, H. E., De Maerschalck, B., Van Oyen, T., van der Vegt, M., & van der Wegen, M. (2019). Closure of secondary basins causes channel deepening in estuaries with moderate to high friction. *Geophysical Research Letters*, *46*(22), 13209–13216. https://doi.org/10.1029/2019GL084444
Percy, K. L., Bella, D. A., Sutterlin, C., & Clingman, P. C. (1974). *Description and information sources for Oregon estuaries* (p. 294). Corvallis, OR: Sea Grant College Program.
Ralston, D. K., & Geyer, W. R. (2009). Episodic and long-term sediment transport capacity in the Hudson River estuary. *Estuaries and Coasts*, *32*(6), 1130.
Ralston, D. K., & Geyer, W. R. (2019). Response to channel deepening of the salinity intrusion, estuarine circulation, and stratification in an urbanized estuary. *Journal of Geophysical Research: Oceans*, *124*(7), 4784–4802. https://doi.org/10.1029/2019JC015006
Ralston, D. K., Geyer, W. R., Traykovski, P. A., & Nidzieko, N. J. (2013). Effects of estuarine and fluvial processes on sediment transport over deltaic tidal flats. *Continental Shelf Research*, *60*, S40–S57.
Ralston, D. K., Geyer, W. R., & Warner, J. C. (2012). Bathymetric controls on sediment transport in the Hudson River estuary: Lateral asymmetry and frontal trapping. *Journal of Geophysical Research*, *117*(C10). https://doi.org/10.1029/2012JC008124
Robbins, W. G. (1984). Timber town: Market economics in Coos Bay, Oregon, 1850 to the present. *The Pacific Northwest Quarterly*, *75*(4), 146–155.
Roye, C., 1979. *Natural resources of Coos Bay estuary* (Final Report, Estuary Inventory Project, p. 87). Portland, OR: Oregon Department of Fish and Wildlife.
Rumrill, S. S. (2006). *The ecology of the south slough estuary: Site profile of the south slough national estuarine research Reserve* (p. 238). Charleston, OR: South Slough National Estuarine Research Reserve.
Schulz, E., Grasso, F., Le Hir, P., Verney, R., & Thouvenin, B. (2018). Suspended sediment dynamics in the macrotidal Seine Estuary (France): 2. Numerical modeling of sediment fluxes and budgets under typical hydrological and meteorological conditions. *Journal of Geophysical Research: Oceans*, *123*(1), 578–600. https://doi.org/10.1002/2016JC012638
Slagle, A. L., Ryan, W. B. F., Carbotte, S. M., Bell, R., Nitsche, F. O., & Kenna, T. (2006). Late-stage estuary infilling controlled by limited accommodation space in the Hudson River. *Marine Geology*, *232*(3–4), 181–202.
Sutherland, D. A., & O'Neill, M. A. (2016). Hydrographic and dissolved oxygen variability in a seasonal Pacific Northwest estuary. *Estuarine, Coastal and Shelf Science*, *172*(C), 47–59. https://doi.org/10.1016/j.ecss.2016.01.042
Talke, S. A., Kemp, A. C., & Woodruff, J. (2018). Relative sea level, tides, and extreme water levels in Boston Harbor from 1825 to 2018. *Journal of Geophysical Research: Oceans*, *123*(6), 3895–3914. http://doi.org/10.1029/2017JC013645

Thom, R. M., Borde, A. B., Rumrill, S., Woodruff, D. L., Williams, G. D., Southard, J. A., & Sargeant, S. L. (2003). Factors influencing spatial and annual variability in eelgrass (Zostera marina L.) meadows in Willapa Bay, Washington, and Coos Bay, Oregon, estuaries. *Estuaries*, *26*(4), 1117–1129.

Townend, I. H., Wang, Z. B., & Rees, J. G. (2007). Millennial to annual volume changes in the Humber Estuary. *Proceedings of the Royal Society A: Mathematical, Physical & Engineering Sciences*, *463*(2079), 837–854. http://doi.org/10.1098/rspa.2006.1798

Umlauf, L., Burchard, H., & Hutter, K. (2003). Extending the k-[omega] turbulence model towards oceanic applications. *Ocean Model*, *5*(3), 195–218. https://doi.org/10.1016/S1463-5003(02)00039-2

Uncles, R. J., & Smith, R. E. (2005). A note on the comparative turbidity of some estuaries of the Americas. *Journal of Coastal Research*, 845–852.

Uncles, R. J., Stephens, J. A., & Smith, R. E. (2002). The dependence of estuarine turbidity on tidal intrusion length, tidal range and residence time. *Continental Shelf Research*, *22*(11–13), 1835–1856.

U.S. Army Corps of Engineers (USACE). (2015). *Coos Bay federal navigation channel and Charleston side channel dredging project: Sediment quality evaluation report*. Portland, OR: Sediment Quality Team (CENWP-EC-HR).

Van Dyke, E., & Wasson, K. (2005). Historical ecology of a central California estuary: 150 Years of habitat change. *Estuaries*, *28*(2), 173–189. http://doi.org/10.1007/BF02732853

van Maren, D. S., Oost, A. P., Wang, Z. B., & Vos, P. C. (2016). The effect of land reclamations and sediment extraction on the suspended sediment concentration in the Ems Estuary. *Marine Geology*, *376*, 147–157.

van Maren, D. S., van Kessel, T., Cronin, K., & Sittoni, L. (2015). The impact of channel deepening and dredging on estuarine sediment concentration. *Continental Shelf Research*, *95*(C), 1–14. http://doi.org/10.1016/j.csr.2014.12.010

van Maren, D. S., Winterwerp, J. C., & Vroom, J. (2015). Fine sediment transport into the hyper-turbid lower Ems River: the role of channel deepening and sediment-induced drag reduction. *Ocean Dynamics*, *65*(4), 589–605.

van Rijn, L., & Grasmeijer, B. (2018). Effect of channel deepening on tidal flow and sediment transport—Part II: muddy channels. *Ocean Dynamics*, *68*(11), 1481–1501.

Warner, J. C., Sherwood, C. R., Signell, R. P., Harris, C. K., & Arango, H. G. (2008). Development of a three-dimensional, regional, coupled wave, current, and sediment-transport model. *Computers & Geosciences*, *34*(10), 1284–1306.

Winterwerp, J. C. (2001). Stratification effects by cohesive and noncohesive sediment. *Journal of Geophysical Research*, *106*, 22559–22574.

Winterwerp, J. C. (2011). Fine sediment transport by tidal asymmetry in the high-concentrated Ems River: Indications for a regime shift in response to channel deepening. *Ocean Dynamics*, *61*(2–3), 203–215.

Winterwerp, J. C., Wang, Z. B., van Braeckel, A., van Holland, G., & Kösters, F. (2013). Man-induced regime shifts in small estuaries—II: A comparison of rivers. *Ocean Dynamics*, *63*(11–12), 1293–1306. http://doi.org/10.1007/s10236-013-0663-8

Yellen, B., Woodruff, J. D., Ralston, D. K., MacDonald, D. G., & Jones, D. S. (2017). Salt wedge dynamics lead to enhanced sediment trapping within side embayments in high-energy estuaries. *Journal of Geophysical Research: Oceans*, *122*(3), 2226–2242. https://doi.org/10.1002/2016JC012595

## References From the Supporting Information

Asselman, N. E. M. (2000). Fitting and interpretation of sediment rating curves. *Journal of Hydrology*, *234*(3–4), 228–248.

Walling, D. E. (1977). Assessing the accuracy of suspended sediment rating curves for a small basin. *Water Resources Research*, *13*, 531–538.